UNIVERSITY OF OKLAHOMA

GRADUATE COLLEGE

A HIGHLY STABLE AND REPEATABLE SOURCE FOR SPECTROSCOPY OF THE $BO_u^+ \leftarrow XO_g^+$ TRANSITIONS IN $^{130}Te_2$

A THESIS

SUBMITTED TO THE GRADUATE FACULTY

in partial fulfillment of the requirements for the

Degree of

MASTER OF SCIENCE

By

DAVID S. LA MANTIA
Norman, Oklahoma
2014

A HIGHLY STABLE AND REPEATABLE SOURCE FOR SPECTROSCOPY OF THE $BO_u^+ \leftarrow XO_g^+$ TRANSITIONS IN $^{130}Te_2$

A THESIS APPROVED FOR THE
HOMER L. DODGE DEPARTMENT OF PHYSICS AND ASTRONOMY

BY

[redacted]

Dr. John Moore-Furneaux, Chair

[redacted]

Dr. Gregory Parker

[redacted]

Dr. Eric R. I. Abraham

Contents

Abstract

Presented here is the detailed discussion of the use of a stabilized helium-neon laser in a Fabry-Perot interferometer to create a highly stable, precise, and repeatable frequency reference source for use in spectroscopy. Tellurium ($^{130}Te_2$) was scanned from 664 THz to 676 THz with a tunable diode laser. Spectra lines were then identified for the $BO_u^+ \leftarrow XO_g^+$ transitions in this molecule. From this many high order spectroscopic constants were determined.

1 Introduction

The electronic spectra of $^{130}Te_2$ serves as a wavelength standard for many new spectroscopic investigations. The molecule is also of interest for a new gain medium for optically pumped lasers, as well as relativistic investigations of large spin-orbit coupling. Tellurium has been spectroscopically studied since the 1960s [Jha et al., 1969] [Balasubramanian and Ravimohan, 1987], and a published atlas has been available since the 1970s [Cariou and Luc, 1980]. While novel at the time, this atlas has since been rendered highly imprecise due to the presence of Doppler broadening. Using Doppler-free techniques, the linewidths of transitions are much less than the Doppler width of $\sim$ 10 Hz. Laser induced fluorescence spectroscopy was used in spectroscopy for tellurium [Stone and Barrow, 1975] [Verges et al., 1982] [Topouzkhanian et al., 1985], but this technique has been limited to $\sim$ 1500 cm^{-1} which was insufficient for an effective study of the $B0_u^+$ band.

The frequency difference between a line position and a high-finesse cavity mode is used as a frequency reference [Courteille et al., 1994] [Scholl et al., 2005] [Gillaspy and Sansonetti, 1991]. Our laboratory used this technique to record the spectra of $^{130}Te_2$ from 664 THz to 676 THz using a tunable diode laser. The scanning laser was coupled into a cavity that is locked to a stabilized reference laser. The resulting transmission resonances were then recorded. This recording gives an effective frequency ruler that was recorded along with the tellurium saturated absorption spectra. The position of the D1 $6P_0 \leftarrow 6S$ hyperfine lines in the ground state of caesium was used as an absolute frequency reference, and the line spectra were used to independently measure the cavity free spectral range. Finally, the stability of this system was determined by repetitively scanning a Cs D1 line.

Rotational analysis of the $B0_u^+ \leftarrow X0_g^+$ transitions in tellurium has been

theoretically modelled and analyzed [Effantin et al., 1980]
[Barrow and du Parcq, 1972] [Yee and Barrow, 1972]. Spectroscopic constants for the ground state of $^{130}Te_2$ have been previously determined [Verges et al., 1982]. Using these constants, we fit $B0_u^+ \leftarrow X0_g^+$ transitions using an iterative computer algorithm. This was done for both P and R branches to J values on the order of 100. From this spectroscopic constants for the $B0_u^+$ state were determined.

2 Experimental Details

2.1 Saturated Absorption Spectroscopy of Tellurium

2.1.1 Frequency Reference

The blue light used to produce transitions in $^{130}Te_2$ comes from a frequency doubled IR laser (Toptica TA-SHG Pro). Within this laser the primary oscillator is an IR diode laser. This IR light is amplified and then doubled by a beta-barium-borate (BBO) crystal in a cavity. A portion of the IR laser light is picked off using a fiber coupler behind a partially transmissive mirror to create a frequency reference ruler [Fig. 1].

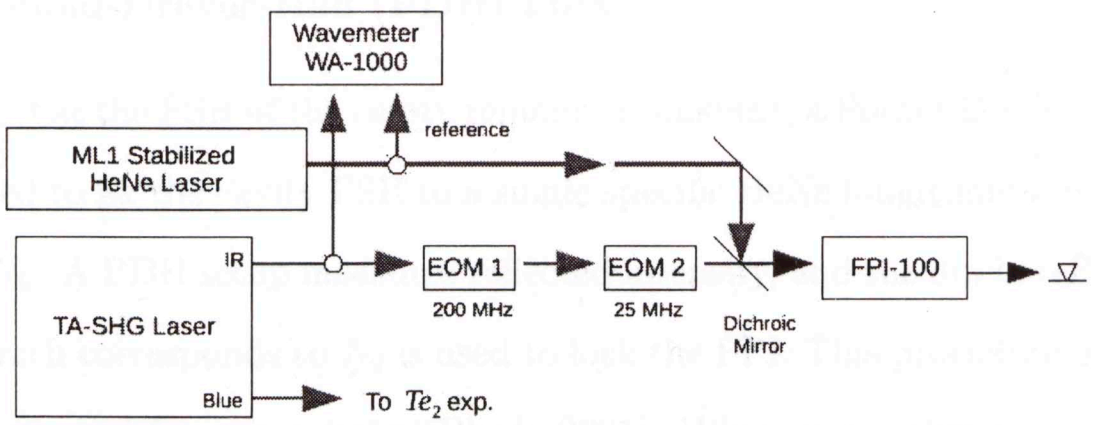

Figure 1: Frequency Marker Setup

The light is sent first through two electric-optic phase modulators (EOMs)

set at 200 MHz and 25 MHz. Both are referenced to a GPS disciplined radio frequency (RF) source. This creates major sidebands on the main IR laser line at 200 MHz spacing, with subsidiary sidebands at 25 MHz spacing to create an effective frequency "ruler" [Fig. 2]. As a result high relative accuracy is achieved because the RF sources are disciplined to $1/10^9$. A stabilized HeNe laser (μg ML-1), $\Delta f/f < 1/10^9$, is used as a reference for a wavemeter (Burleigh WA-1000), which is accurate to 100 MHz. This HeNe light is also used to lock a Fabry-Perot interferometer (FPI) (Toptica FPI-100) to a single longitudinal mode. The IR beam is also coupled to the FPI and the IR transmission is measured by a photodiode and recorded. A bias-lock on the 200 MHz EOM gives the desired relative sideband intensities, as shown. This pattern allows easier computer identification of the markers. The free spectral range (FSR) of the mode-matched confocal cavity is approximately 2 GHz, but the cavity coupling is changed slightly so that it is non-mode matched to create alternating larger and smaller markers approximately every 1 GHz in the absence of added sidebands [Fig. 3]. As the blue is generated by doubling the IR, these markers also serve as a frequency axis for the $^{130}Te_2$ spectra.

2.1.2 Pound-Drever-Hall (PDH) Lock

To ensure that the FSR of the cavity remains a constant, a Pound-Drever-Hall lock is employed to fix the cavity FSR to a single specific HeNe longitudinal mode that we label N_0. A PDH setup measures reflected intensity, and the dip in reflected intensity which corresponds to N_0 is used to lock the FPI. This procedure decouples the intensity and frequency noise [Black, 2001]. When one wishes to analyze the reflection off a cavity, the intensity alone is inappropriate as it is symmetric. The derivative is anti-symmetric, and this is achieved by modulating the frequency a small amount with respect to the FSR of the cavity. Above resonance, the deriva-

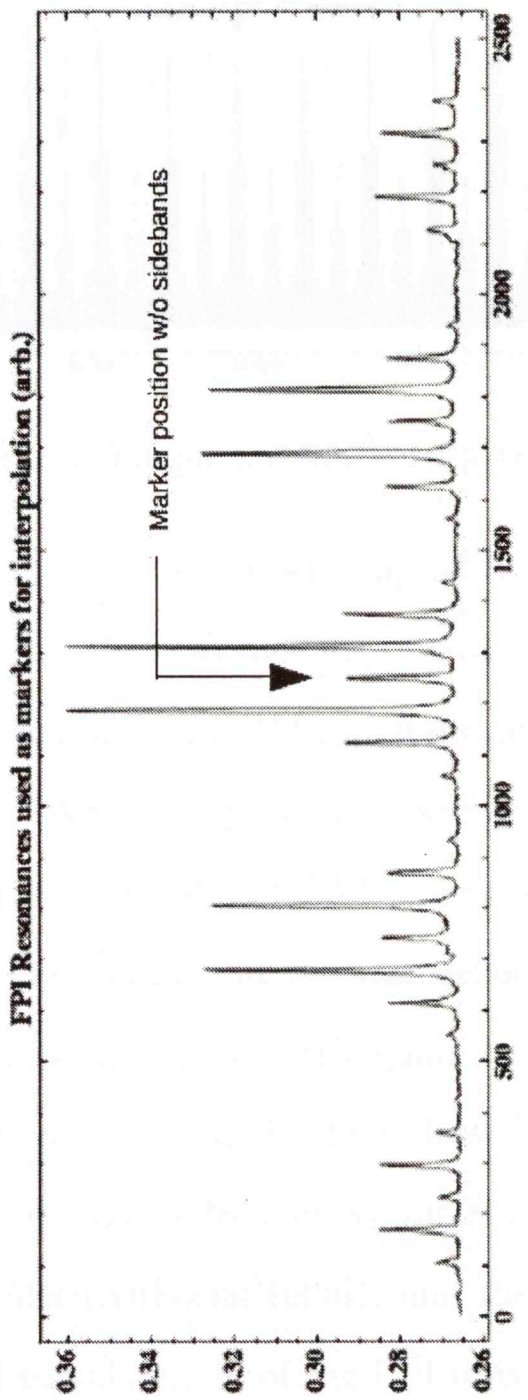

Figure 2: Single Set of Frequency Markers

tive of the reflected intensity is positive with respect to the laser frequency and a small variation will cause the reflected intensity to oscillate sinusoidally in phase with the modulation frequency. Below resonance, the derivative is negative and the intensity will oscillate sinusoidally out of phase (180°) with the modulation frequency. Comparison of the modulation frequency and variation in the reflected intensity indicates what side of resonance the laser is on.

A fiber coupler sends the HeNe laser to the wavemeter for a frequency reference,

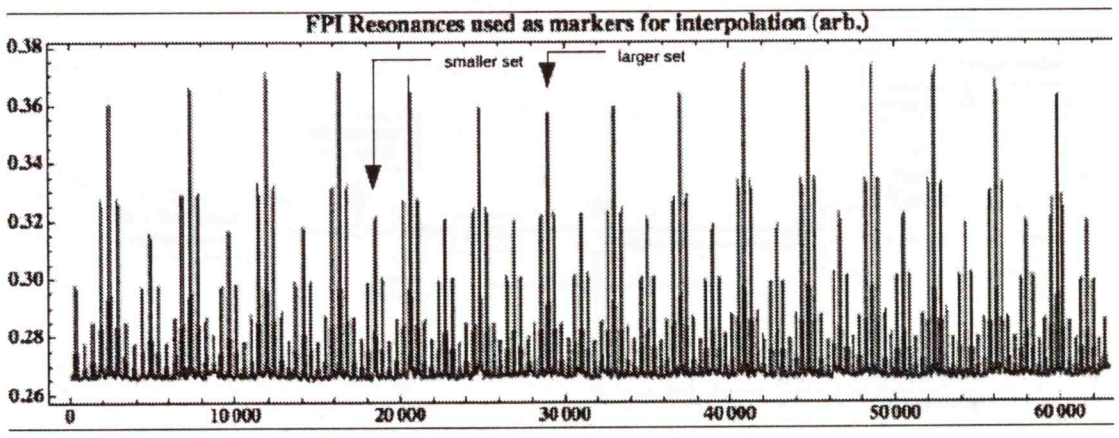

Figure 3: Frequency Marker Pattern

as discussed, and towards the FPI. The fiber coupled HeNe laser emission is split in two. One portion is used as the reference for the wavemeter. The other part is sent through a linear polarizer and an EOM which produces the needed frequency modulation at $\sim$ 0.5 MHz. After the EOM it is sent though a polarizing beam splitter (PBS) and a quarter-wave plate (QWP) to produce circularly polarized light. After reflection off the cavity and retransmission through the QWP, the light is once again linearly polarized but orthogonal to the incoming light. The PBS now directs this light to a photodiode. In a classic PDH setup this feedback would be sent to the laser to vary its frequency, but our feedback is demodulated and sent to a servo controller (NuFocus 1000B) and then on to the piezoelectric transducer (PZT) coupled to one mirror of the FPI to control the cavity's length. This effectively controls the FSR of the cavity.

The PZT's voltage is also sent to a LabView program which controls the temperature of the aluminum body of the FPI. LabView then controls a thermo-electric heater-cooler (TEHC) to change the temperature of the aluminum and drive the voltage on the PZT to zero. The same oscillator used to drive an EOM is referenced to the servo to lock the cavity. This creates a robust lock on the N_0 mode of the cavity that, to date, has rarely broken [Fig. 4]. Furthermore, the lock can be restored reproducibly to N_0.

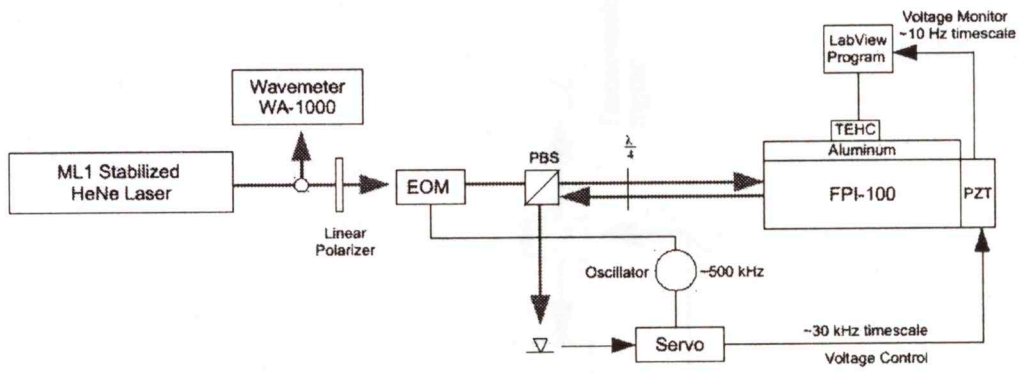

Figure 4: PDH Setup

2.1.3 Scanning Tellurium

The experimental set up for scanning the tellurium is known as saturated absorption spectroscopy [Fig. 5]. The doubled diode laser produces linearly polarized light and a half-wave plate (HWP) is used to rotate the polarization before the light strikes a PBS. This splits the beam and allows control of the ratio of deflected (probe) and undeflected (pump) beams. The current to the tapered amplifier and a HWP inside the diode laser setup are used to set the power at roughly 80 mW, which has been found empirically to be sufficient to saturate most of the $^{130}Te_2$ transitions without undue distortion. An exterior HWP is used to reduce the probe beam as much as possible.

The pump beam is sent through and electro-optic amplitude modulator (EOAM) referenced at around 30 kHz and on through a QWP and HWP. The combination of these creates linearly polarized light whose linear polarization is rotating at the reference frequency. Combining this with a PBS creates an electro-optic chopper. The PBS dumps one of the directions of polarized light (not shown) and creates linearly polarized light whose amplitude is oscillating at a controllable frequency and modulation depth. The pump then passes through the tellurium oven set at 650 °C and strikes a photodiode. This transmission data is then recorded by a

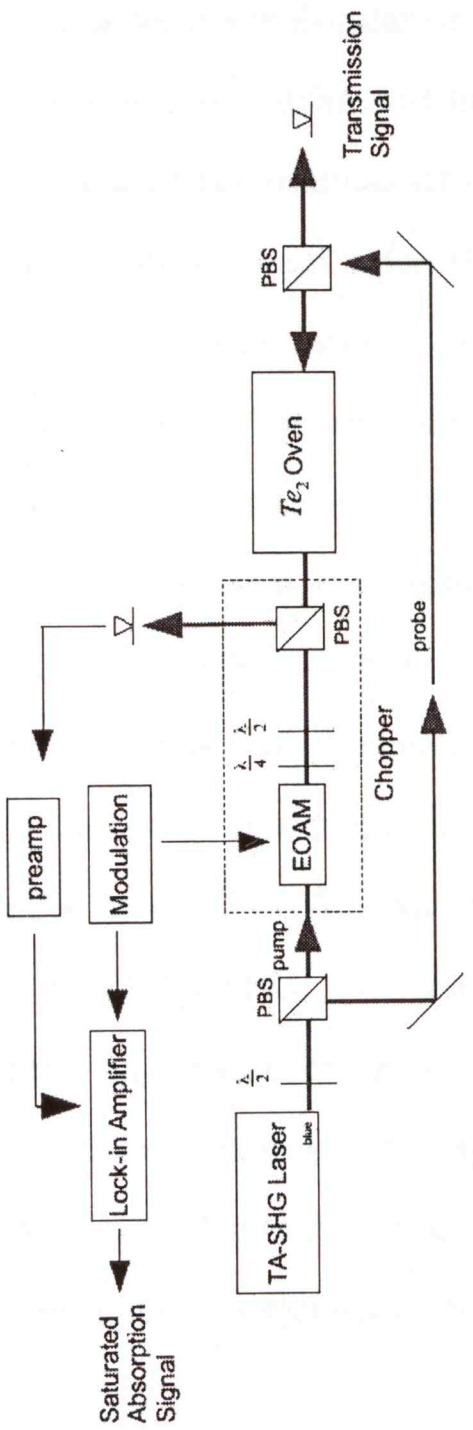

Figure 5: Saturated Absorption Setup

computer.

The probe beam is deflected around the Te oven and back through the $^{130}Te_2$. Irises reduce the probe beam so that it passes entirely within the pump beam. This saturated absorption data is also recorded by a photodiode and computer. By passing the beams along counter-propagating axes, the Doppler effect is essentially eliminated and the probe records the lifetime limited bandwidths as evidenced by the essentially pure Lorentzian lineshapes of the resulting spectra.

When a strong beam interacts with a molecular or atomic system, the Doppler width is generally larger than the line widths and fine details of the spectrum. Directing a weak probe beam against the original strong pump beam causes little change in the absorption of the probe beam since the pump beam has already saturated most transitions. Both beams interact with atomic velocity groups arranged symmetrically along the beam line and the Doppler width in the probe beam is essentially eliminated. The population hole caused by the pump beam is larger than that of the probe beam so that the probe absorption gives an image of the strong field hole. Since this is an absorber, a maximum appears in the transmission. The probe beam is weak and thus feels the full effect of the strong field transmission and has little power broadening [Stenholm, 1984].

A field-programmable gate array (FPGA) (National Instruments) electronically sweeps the frequency of the TA-SHG. The frequency was scanned up and down over its range to identify any frequency skips and simultaneously recorded by LabView on a computer. A typical scan covered approximately 30 GHz in the IR (60 GHz blue) and took about 22 minutes [Fig. 6]. This setup was used to scan all 12 THz of $^{130}Te_2$ from optical frequencies 664 THz to 676 THz.

2.2 Infrared Scanning Of Caesium

As previously discussed, the wavemeter has a resolution of only about 100 MHz. Creation of the markers creates good relative accuracy, but a precise absolute frequency source is also needed. Fortunately, the D1 $6P_0 \leftarrow 6S$ hyperfine split transitions in ^{133}Cs are in the IR range of our $^{130}Te_2$ scans. These are given as:

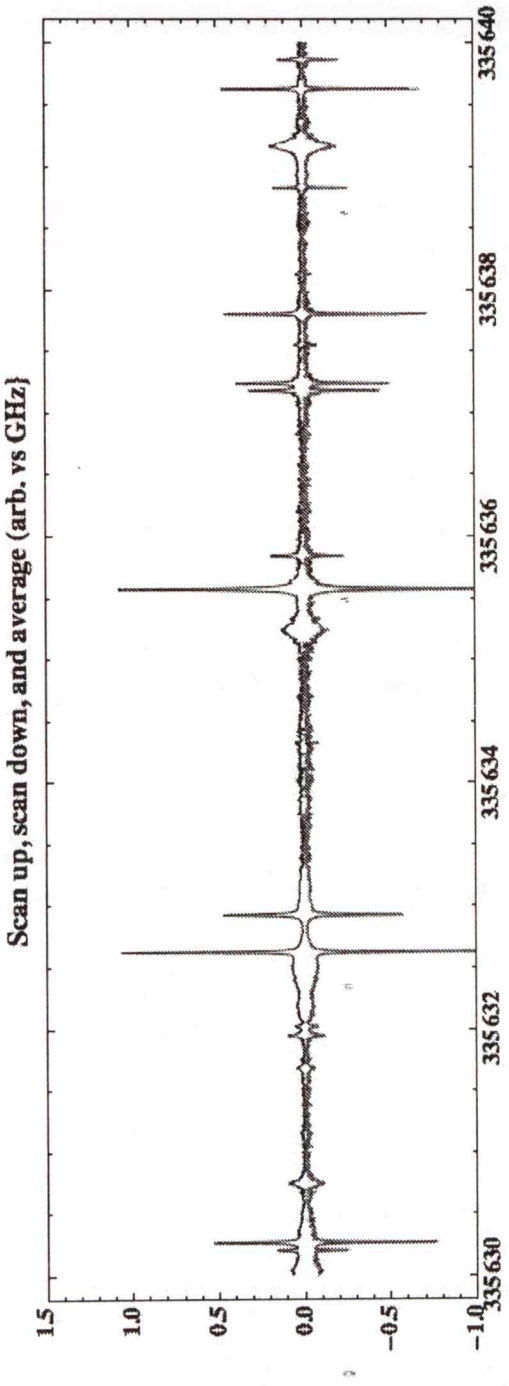

Figure 6: Example Scan

335111370129.1(3.4)kHz

335112537852.7(3.3)kHz

335120562760.8(3.4)kHz

335121730484.4(3.3)kHz

[Gerginov et al., 2006] [Fig. 7]

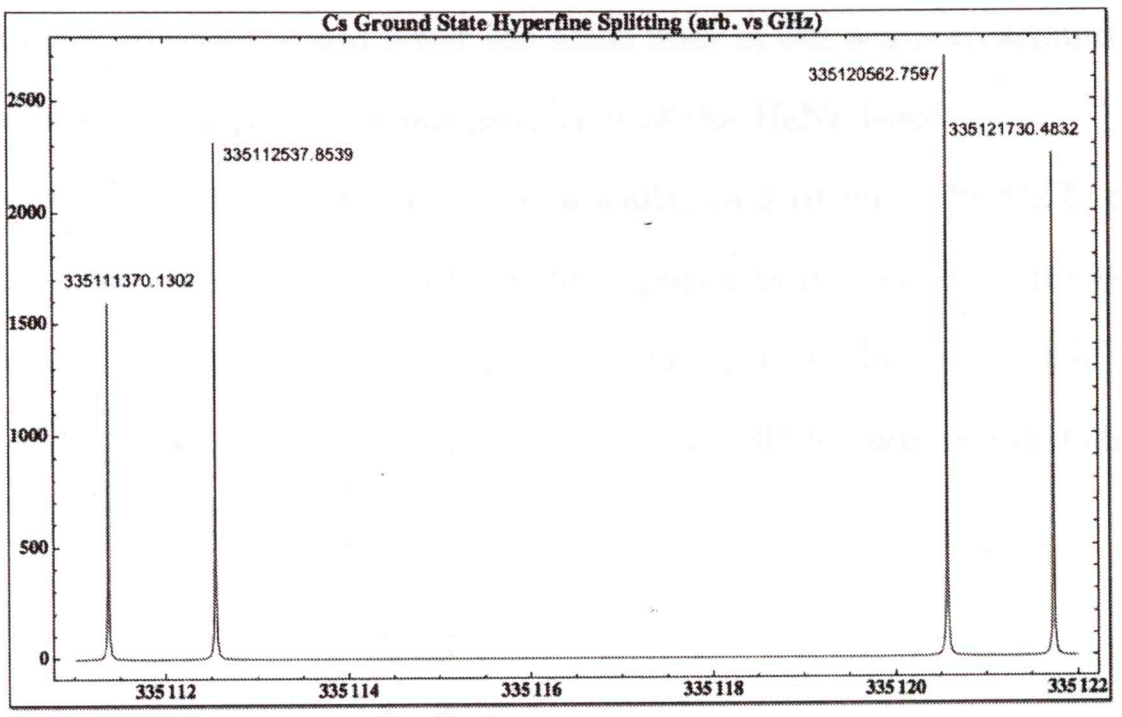

Figure 7: Reference

Having this frequency source serves three purposes. The first is that is gives us an absolute frequency for our frequency ruler. The second is that it allows us to precisely measure our FSR independently. The third is that is allows us to measure the stability of our system. A similar HeNe setup to that described above for $^{130}Te_2$ is used [Fig. 8]. Now our markers and frequency sweeps are not precise or accurate enough. Thus, only the wide bandwidth (30 GHz) waveguide EOM is used to create a single sideband on either side of the main IR laser line. A PDH configuration is once again employed to lock one of these sidebands to the HeNe stabilized FPI. A GPS disciplined RF synthesizer is then used to scan the main laser line over a single caesium transition while continuously keeping the IR sideband locked to the FPI.

A single transition was scanned several thousand times over more than two days to evaluate the Allan deviation [Fig. 9]. Allan deviation (or variance) is a time domain based analysis technique developed to study the frequency stability of oscillators and has been used to identify stochastic processes such as quantization and white noise [Allan, 1966] [Niu et al., 2014]. It was then determined that

approximately 30 scans would lower the noise floor of our scans to around 50 kHz, consistent with the reported Allan deviation of the HeNe laser.

The servo controller could be systematically used to push the PZT, and thus the cavity, onto other HeNe cavity modes. This was done from a range of ± 50 HeNe modes from N_0. By measuring the difference in the position of the FPI resonant sidebands to the caesium transitions, a FSR for our zeroth mode could be deduced [Fig. 10].

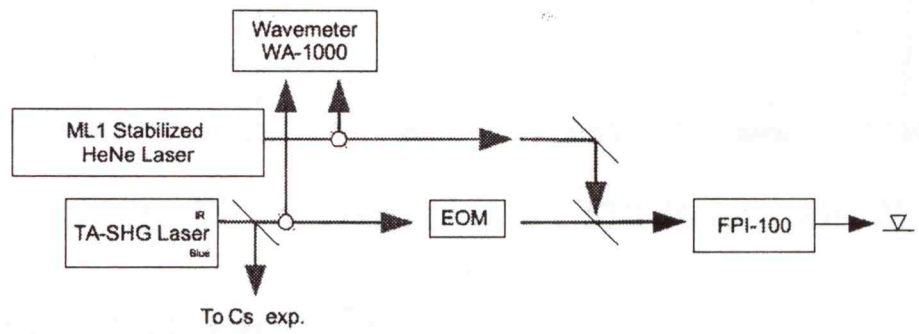

Figure 8: Cs Experimental Configuration

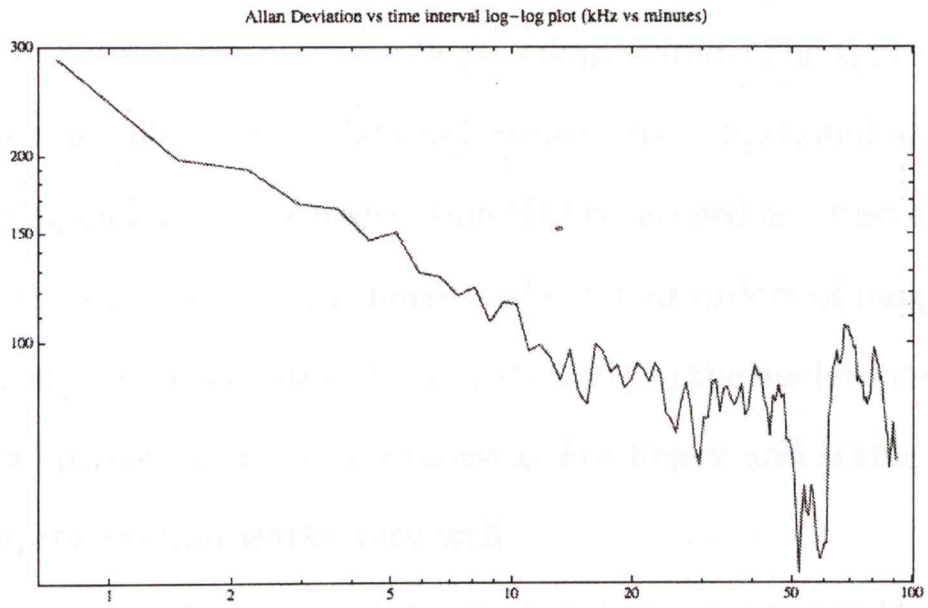

Figure 9: Allan Deviation vs. time (log-log)

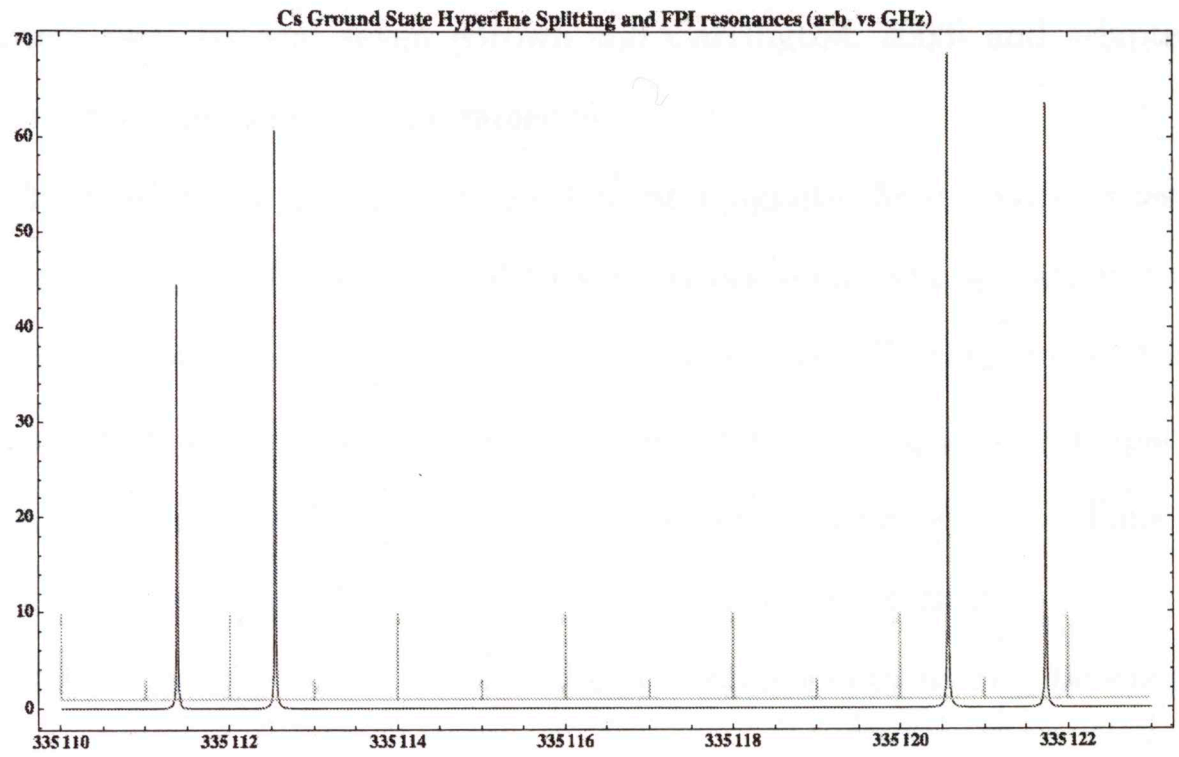

Figure 10: D1 Cs Transitions w/ FPI Resonances N_0

3 Theoretical Details

A molecule is a collection of positively charged nuclei and negatively charged electrons bound by the the Coulomb force. Even when treated classically, the motion of these systems can be exceedingly complicated. The types of motion can be broken down as follows: translational, rotational, vibrational and electronic.

The Born-Oppenheimer approximation (B-Oa) is used as a first approximation. It states that, because the nucleus mass is about four orders of magnitude greater than the electron, over a very short time scale (10^{-6} s) the nucleus may be regarded as stationary while the electrons are moving. For heavy and stable molecules like $^{130}Te_2$, this approximation works very well.

Kinetic and potential energy will be analyzed to move towards an appropriate Hamiltonian for $^{130}Te_2$. Relevant approximations will be made to allow separation of vibrational and rotational energies. This will lead to a description of the transition energies for a given vibrational and rotational level for the $B0_u^+ \leftarrow X0_g^+$ band. All theoretical work is rooted by work set forth by Brown and Carrington

in chapters two, six and seven [Brown and Carrington, 2003] and adapted to a symmetric homonuclear bosonic molecule.

In the absence of an external electric or magnetic field, space is isotropic. Translation of a body from one point to another is a symmetry operation; therefore translational motion may be rigorously separated from all other types of motion. This separation is achieved by moving the arbitrary origin or our space-fixed coordinate system to a fixed origin at the molecule center of mass. Thus, as the molecule moves through the lab frame, the origin moves with it.

The kinetic energy of the nuclei and the orbiting electrons may be easily written:

$$T = -\hbar^2 \sum_{\alpha=1}^{2} \frac{1}{2M_\alpha} \nabla_\alpha^2 - \hbar^2 \sum_{i=1}^{n} \frac{1}{2m_i} \nabla_i^2$$

The α term represents the nuclei and the i term represents the electrons. This form may be transformed so that the translational, vibrational, rotational, and electronic terms are separated. First it is useful to consider a translation of the coordinate system. A transformation to the molecule center of mass (COM) will allow translational motion to be rigorously separated. A transformation to the center of mass of the two nuclei is useful for considering the coupling of electronic and nuclear motion.

3.1 Center of Mass (COM)

Transformation to the center of mass of the molecule is considered here, so that translational motion can be rigorously separated [Fig. 11]. The vector $\mathbf{R_0}$ to the center of mass of the molecule is given as:

$$\mathbf{R}_0 = \frac{1}{M}\{m \sum_i \mathbf{R}_i + \sum_\alpha M_\alpha \mathbf{R}_\alpha\}$$

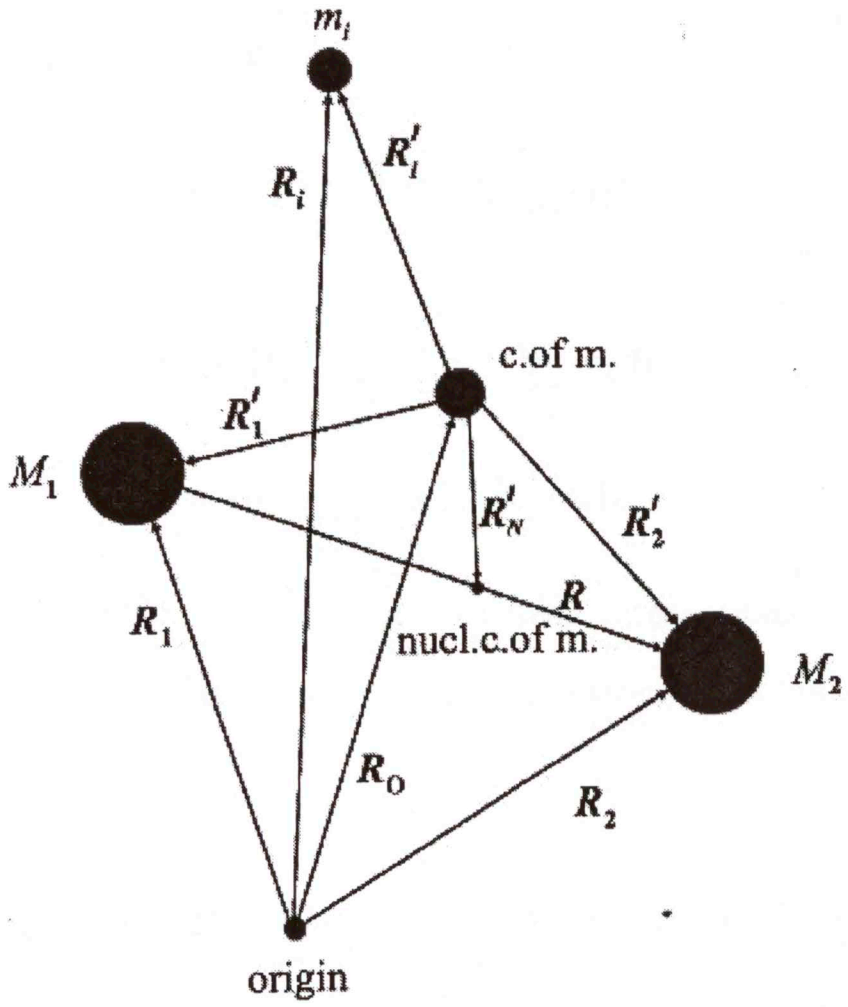

Figure 11: Change of Coordinates [Brown and Carrington, 2003, Fig. 2.1]

where M is the total mass of all particles. After transformation, the kinetic energy may be written as:

$$T = \frac{1}{2M}\mathbf{P}_0^2 + \frac{1}{2\mu}\mathbf{P}_R^2 - \frac{1}{2M}\sum_{i,j=1}^{n}\mathbf{P}_i' \cdot \mathbf{P}_j' + \frac{1}{2m_e}\sum_{i=1}^{n}\mathbf{P}_i'^2$$

where μ is the reduced nuclear mass and $\mathbf{R}_i' = \mathbf{R}_i - \mathbf{R}_0$. The first term represents the translational kinetic energy of the whole molecule and may be omitted in field-free space due to translational symmetry in isotropic space. The second term is the nuclei's kinetic energy. The third term is the mass polarization and describes the small fluctuations in the position of the center of mass as the electrons move around within the molecule. The last term is the kinetic energy of the individual electrons.

Transformation from the center of mass of the molecule to the center of mass of the nuclei, which is located at:

$$\mathbf{R}_N^{'} = \frac{1}{M_1 + M_2} \sum_{\alpha} M_\alpha \mathbf{R}_\alpha^{'}$$

$$\mathbf{R}_i^{''} = \mathbf{R}_i^{'} - \frac{1}{M_1 + M_2} \sum_{\alpha} M_\alpha \mathbf{R}_\alpha^{'}$$

$$= \mathbf{R}_i^{'} + \frac{1}{M_1 + M_2} \sum_{i} m_i \mathbf{R}_i^{'}$$

is considered here so that electronic and nuclear interactions may be coupled. Transforming our corresponding momentum operators gives us the new kinetic energy operator:

$$T = \frac{1}{2M}\mathbf{P}_0^2 + \frac{1}{2\mu}\mathbf{P}_R^2 + \frac{1}{2(M_1 + M_2)} \sum_{i,j} \mathbf{P}_i^{''} \cdot \mathbf{P}_j^{''} + \frac{1}{2m} \sum_{i} \mathbf{P}_i^{''2}$$

These terms represent the kinetic energy due to translation, the nuclei, the electrons and finally a correction term, respectively. This correction term is the previously mentioned mass polarization term.

3.2 Total Hamiltonian in Free Space

The following considerations will take the origin of the coordinate system to be the center of mass of the two nuclei. Setting aside the translational motion of the molecule, we may use the previous equation in differential form to represent the kinetic energies of the nuclei and electrons. Terms representing the potential energy, electron spin interactions and nuclear spin interactions are then added to form our Hamiltonian.

$$\mathcal{H}_T = \mathcal{H}_{el} + \mathcal{H}_{nucl}$$

$$\mathcal{H}_{el} = -\frac{\hbar^2}{2m}\sum_i \nabla_i^2 - \frac{\hbar^2}{2M_N}\sum_{i,j}\nabla_i\cdot\nabla_j + \sum_{i<j}\frac{e^2}{4\pi\epsilon_0 R_{ij}}$$

$$-\sum_{\alpha,i}\frac{Z_\alpha e^2}{4\pi\epsilon_0 R_{i\alpha}} + \mathcal{H}(\mathbf{S}_i) + \mathcal{H}(\mathbf{I}_\alpha)$$

$$\mathcal{H}_{nucl} = -\frac{\hbar^2}{2\mu}\nabla_R^2 + \sum_{\alpha,\beta}\frac{Z_\alpha Z_\beta e^2}{4\pi\epsilon_0 R}$$

The nuclear interaction Hamiltonian $\mathcal{H}(\vec{I_\alpha})$ is included in the electronic Hamiltonian since its most significant effects arise from electronic motion interactions. The electron spin interaction Hamiltonian $\mathcal{H}(\vec{S_i})$ is derived from relativistic quantum mechanics. The electron-electron, electron-nuclear and the purely nuclear electrostatic repulsion potentials have been included.

3.3 Rotational Motion

It becomes more convenient to use curvilinear coordinates to describe the rotational motion of the nuclei, namely Euler's angles [Fig. 12]. The transformation between the space- and molecule-fixed coordinate system is :

$$\begin{pmatrix} X \\ Y \\ Z \end{pmatrix} = \mathcal{M}\begin{pmatrix} x \\ y \\ z \end{pmatrix}$$

where $\mathcal{M}$ is the following unitary matrix:

$$\begin{pmatrix} \cos\phi\cos\theta\cos\chi - \sin\phi\sin\chi & -\sin\phi\cos\chi - \cos\phi\cos\theta\sin\chi & \cos\phi\sin\theta \\ \sin\phi\cos\theta\cos\chi + \cos\phi\sin\chi & \cos\phi\cos\chi - \sin\phi\cos\theta\sin\chi & \sin\phi\sin\theta \\ -\sin\theta\cos\phi & \sin\theta\sin\chi & \cos\theta \end{pmatrix}$$

The third Euler angle χ is redundant since the internuclear distance R supplies the third coordinate needed to define our nuclear coordinates. This allows the

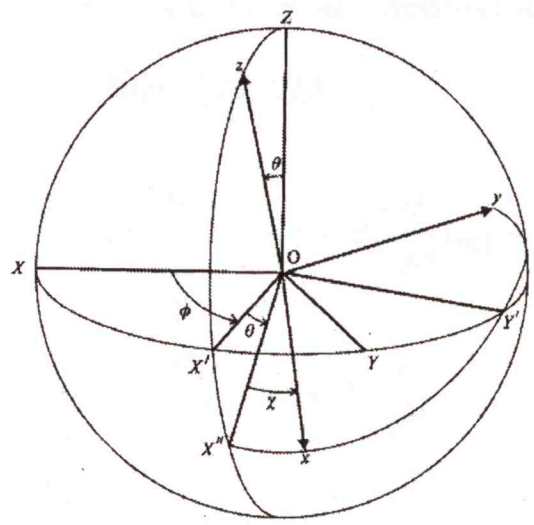

Figure 12: Euler Angles[Brown and Carrington, 2003, Fig. 2.2]

nuclear Hamiltonian to be redefined in the space-fixed coordinate system.

$$\mathcal{H}_{nucl} = -\frac{\hbar^2}{2\mu R^2}\{\frac{\partial}{\partial R}(R^2\frac{\partial}{\partial R}) + \csc\theta\frac{\partial}{\partial\theta}(\sin\theta\frac{\partial}{\partial\theta})$$

$$+ \csc^2\theta(\frac{\partial^2}{\partial\phi^2} + \frac{\partial^2}{\partial\chi^2} - 2\cos\theta\frac{\partial^2}{\partial\phi\partial\chi})\} + \mathcal{V}_{nucl}(R)$$

If we define the total electronic angular momentum $\hbar\mathbf{M}$ by

$\mathbf{M} = \mathbf{L} + \mathbf{S}$ we can redefine partial differential operators between the space-fixed (s) and molecule-fixed (m) coordinate system

[Brown and Carrington, 2003, Eqs. 89-91]:

$$(\frac{\partial}{\partial\phi})_s = (\frac{\partial}{\partial\phi})_m - i\cos\theta M_z + i\sin\theta\cos\chi M_x - i\sin\theta\sin\chi M_y$$

$$(\frac{\partial}{\partial\theta})_s = (\frac{\partial}{\partial\theta})_m - i\sin\chi M_x - i\cos\chi M_y$$

$$(\frac{\partial}{\partial\chi})_s = (\frac{\partial}{\partial\chi})_m - iM_z$$

This leads to

$$\mathcal{H}_T = -\frac{\hbar^2}{2\mu R^2}\frac{\partial}{\partial R}(R^2\frac{\partial}{\partial R}) + \frac{\hbar^2}{2\mu R^2}(\mathbf{J}-\mathbf{M})^2 + \mathcal{V}_{nucl}(R)$$

where the molecule-fixed components of **J** are defined as [Brown and Carrington, 2003, Eqs. 121-123]:

$$J_x = -i\{\cos\chi[(\cot\theta\frac{\partial}{\partial\chi})_m - \csc\theta(\frac{\partial}{\partial\phi})_m] + \sin\chi(\frac{\partial}{\partial\theta})_m\}$$

$$J_y = -i\{\sin\chi[(\cot\theta\frac{\partial}{\partial\chi})_m - \csc\theta(\frac{\partial}{\partial\phi})_m] + \cos\chi(\frac{\partial}{\partial\theta})_m\}$$

$$J_z = -i(\frac{\partial}{\partial\chi})_m$$

Having defined our total electronic angular momentum operator **M**, we can say [Brown and Carrington, 2003, Eq. 128]:

$$M_z\psi_e^n(\mathbf{r}_i, R) = \Omega_n\psi_e^n(\mathbf{r}_i, R)$$

where Ω_n is the projection of the total electronic angular momentum along the internuclear axis.

The B-Oa allows us to separate the wave equation for our system. This is highly appropriate for diatomic molecules in a closed shell state like $^{130}Te_2$. This also means that the electronic states do not mix.

$$\Psi_{rve}^0 = \psi_e^n(\mathbf{r}_i, R)\phi_{rv}^n(R, \phi, \theta)$$

The variational principle may be used to arrive at a choice for the function ϕ_{rv}^n. Minimizing the energy $\mathcal{E}_{rve}$ with respect to small changes in ϕ_{rv}^n gives

$$\mathcal{E}_{rve} = \int\int \Psi_{rve}^{0*}\mathcal{H}\Psi_{rve}^0 d\mathbf{r}_i d\mathbf{r} \div \int\int \Psi_{rve}^{0*}\Psi_{rve}^0 d\mathbf{r}_i d\mathbf{r}$$

This leads to the relation [Brown and Carrington, 2003, Eq. 2.136]:

$$[E_e^n(R) - \frac{\hbar^2}{2\mu}\int \psi_e^n \bigtriangledown_R^2 \psi_e^n d\mathbf{r}_i + \mathcal{H}_{nucl}]\phi_{rv}^n = \mathcal{E}_{rve}\phi_{rv}^n$$

And [Brown and Carrington, 2003, Eq. 2.141]:

$$\{-\frac{\hbar^2}{2\mu}\bigtriangledown_R^2 + E_e^n(R) + Q_{nn} + M_{nn} - \frac{\hbar^2}{2\mu R^2}(2\Omega_n J_z - \Omega_n^2)$$

$$+\mathcal{V}_{nucl}(R)\}\phi_{rv}^n = \mathcal{E}_{rve}\phi_{rv}^n$$

The first term is the nuclei's kinetic energy and the second term is the electronic energy. The third, fourth and fifth terms represent small adiabatic corrections to the potential energy. They all have a μ^{-1} reduced mass dependence, unlike $\mathcal{V}_{nucl}$. The rotation-vibration wave equation then obeys [Brown and Carrington, 2003, Eq. 2.142]:

$$\{-\frac{\hbar^2}{2\mu}\bigtriangledown_R^2 + E_e^n(R) + \mathcal{V}_{nucl} - \mathcal{E}_{rve}\}\phi_{rv}^n = 0$$

The electronic energies can still solved for. All approximations thus far are appropriate for a homonuclear diatomic molecule.

We can separate the coordinates in ϕ_{rv}^n by writing it as a product.

$$\phi_{rv}^n = \chi^n(R)e^{iM_J\phi}\Theta^n(\theta)e^{ik\chi}$$

where M_J and k are constants taking integral or half-integral values. M_J signifies the component of total angular momentum $\mathbf{J}$ along the space-fixed axis with $2J+1$ values ranging from $-J$ to J. Considering the entire electronic angular momentum $\mathbf{M}$ has previously yielded an eigenvalue equation. From this we can see that

$$J_z\Psi_{rve}^n = M_z\Psi_{rve}^n = \Omega_n\Psi_{rve}^n$$

or

$$J_z \phi_{rv}^n = \Omega_n \phi_{rv}^n$$

and $k = \Omega_n$.

Use of standard separation of variables gives

[Brown and Carrington, 2003, Eqs. 2.146,147]:

$$\{-\frac{\hbar^2}{2\mu}\frac{1}{R^2}\frac{\partial}{\partial R}(R^2\frac{\partial}{\partial R}) + E_e^n(R) + Q_{n,n}(R) + M_{n,n}(R) + V_{nucl}(R)$$

$$+\frac{\hbar^2}{2\mu R^2}\Omega_n^2 + E_{rot}(R)\}\chi^n(R) = 0$$

$$\{-\frac{\hbar^2}{2\mu R^2}\csc\theta\frac{\partial}{\partial\theta}(\sin\theta\frac{\partial}{\partial\theta}) - \frac{\hbar^2}{2\mu R^2}\csc^2\theta(\frac{\partial^2}{\partial\phi^2} + \frac{\partial^2}{\partial\chi^2} - 2\cos\theta\frac{\partial^2}{\partial\phi\partial\chi})$$

$$-\frac{\hbar^2}{2\mu R^2}2i\Omega_n\frac{\partial}{\partial\chi} - E_{rot}(R)\}e^{iM_J\phi}\Theta^n(\theta)e^{i\Omega_n\chi} = 0$$

The first equation governs the vibration motion of the nuclei while the second governs the rotational motion of the molecule-fixed axis system. This leads to the important result for the rotational eigenvalues (energy) of the system [Brown and Carrington, 2003, Eq. 2.151]:

$$E_{rot}(R) = \frac{\hbar^2}{2\mu R^2}\{J(J+1) - \Omega_n^2\}$$

This can be substituted into our equation for the vibrational motion.

3.4 Vibrational Motion

The vibrating rotor wave equation is rewritten as

[Brown and Carrington, 2003, Eq. 2.15:]:

$$\frac{\hbar^2}{2\mu}\frac{1}{R^2}\frac{d}{dR}\frac{d\chi^n(R)}{dR} + \{E_{rve} - V - \frac{\hbar^2}{2\mu R^2}J(J+1)\}\chi^n(R) = 0$$

where V is the potential function. Even in simple cases, the potential term becomes troublesome. The vibrational wave equation is therefore solved by inserting a restricted form based on semi-empirical constants for the rovibrational levels.

Dunham introduced a solution to this potential [Dunham, 1932]. Consider the dimensionless variable ξ defined by:

$$\xi = \frac{R - R_e}{R_e}$$

where R_e is the equilibrium nuclear separation. This transforms the wave equation to:

$$\frac{d^2\psi^n(\xi)}{d\xi^2} + \frac{2\mu R_e^2}{\hbar^2}\{E - V - \frac{\hbar^2}{2\mu R_e^2(1-\xi)^2}J(J+1)\}\psi^n(\xi) = 0$$

where $\psi^n(\xi) = R\chi^n(R)$. A mass-weighted normal coordinate simplifies the problem,

$$Q = \sqrt{\mu}(R - R_e)$$

so that

$$\int_0^\infty \psi^{n*}(Q)\psi^n(Q)dQ = 1$$

The vibrational Hamiltonian is thus:

$$\mathcal{H}_{vib} = -\frac{\hbar^2}{2}\frac{d^2}{dQ^2} + V$$

$$= \frac{1}{2}P_Q^2 + V$$

where P_Q is the momentum conjugate to Q.

The simplest approximation for V is to assume that it is harmonic

$$\mathcal{H}_0 = \frac{1}{2}(P_Q^2 + \lambda Q^2)$$

where $\lambda = (\hbar\gamma)^2$ and $\gamma = \frac{2\pi\nu}{\hbar}$.

The eigenvalues of this equation are well known, with the energy levels given as:

$$E_\nu = (\nu + 1/2)\hbar\omega \qquad \nu = 0, 1, 2, ...$$

$$= (\nu + 1/2)\hbar^2\gamma$$

In practice the anharmonic terms becomes significant, and Dunham analyzed these effects by expanding the potential in terms of an infinite power series. This expansion leads to a solution of the eigenvalue energies in terms of what are called Dunham constants, $Y_{l,m}$ [Gordy and Cook, 1984]:

$$\frac{E_{\nu J}}{h} = \sum_{l,m} Y_{l,m}(\nu + 1/2)^l J^m (J+1)^m$$

$$= Y_{10}(\nu + 1/2) + Y_{20}(\nu + 1/2)^2 + Y_{01}J(J+1)$$

$$+Y_{11}(\nu + 1/2)J(J+1) + Y_{21}(\nu + 1/2)^2 J(J+1)$$

$$+Y_{31}(\nu + 1/2)^3 J(J+1) + Y_{02}J^2(J+1)^2$$

$$+Y_{12}(\nu + 1/2)J^2(J+1)^2 + Y_{03}J^3(J+1)^3 + ...$$

A less cumbersome potential term was introduced by Morse [Morse, 1929]

$$V = D(1 - e^{-\beta(R-R_e)})^2$$

in which D is the dissociative energy of the molecule and β is a constant. The rovibrational levels are given by

$$\frac{E_{\nu,J}}{hc} = \omega_e(\nu + 1/2) - x_e\omega_e(\nu + 1/2)^2 + B_e J(J+1)$$

$$-D_e J^2(J+1)^2 - \alpha_e(\nu+1/2)J(J+1)$$

in which the parameters (cm^{-1}) are given by

$$\omega_e = \frac{\beta}{2\pi c}\sqrt{\frac{2D}{\mu}}, \quad x_e = \frac{hc\omega_e}{4D}, \quad B_e = \frac{\hbar}{4\pi\mu R_e^2 c}$$

$$D_e = \frac{\hbar^3}{16\pi^3\mu^3\omega_e^2 R_e^6 c^3} = \frac{4B_e^3}{\omega_e^2}$$

$$\alpha_e = \frac{3\hbar^2\omega_e}{4\mu R_e^2 D}\left(\frac{1}{aR_e} - \frac{1}{a^2R_e^2}\right) = 6\sqrt{\frac{x_e B_e^3}{\omega_e}} - 6\frac{B_e^2}{\omega_e}$$

These terms ignore small, higher-order corrections given by Dunham. The first term has the form of a pure vibrator in a harmonic potential, the second term is obtained from the potential, the third term is obtained in the treatment of a rigid rotator, the fourth term is from the centrifugal stretching of the rotating molecule and the fifth term allows for change in the average moment of inertia with vibrational excitation.

The total energy can then be written as:

$$E = T_e + G_\nu + F_\nu(J)$$

where T_e is the electronic energy (also known as the bandhead origin), G_ν is the vibrational energy in terms of constants and ν and $F_\nu(J)$ is the rotational energy in terms of ν and J. $F_\nu(J)$ can be expanded to higher order terms that become significant as J rises [Jennings et al., 1987]:

$$F_\nu(J) = B_\nu J(J+1) - D_\nu J^2(J+1)^2 + H_\nu J^3(J+1)^3$$

$$-L_\nu J^4(J+1)^4 + M_\nu J^5(J+1)^5$$

Constants previously mentioned can then be related to each other:

$$Y_{01} \approx B_\nu, \quad Y_{02} = -D_\nu, \quad Y_{03} = H_\nu, \quad Y_{11} = -\alpha_\nu,$$

$$Y_{12} = -\beta_\nu, \quad Y_{21} = \gamma_\nu,$$

$$Y_{10} = \omega_\nu, \quad \text{and} \quad \mathrm{Y}_{20} = -\omega_\nu \mathrm{x}_\nu$$

4 Computational Details

The recording of $^{130}Te_2$ spectra and IR markers with the TA-SHG Pro over $\sim$ 30 GHz was performed through electronic sweeping of the frequency up and then down. This was to eliminate any directional bias, as well as identifying possible frequency skips or laser extinction due to the doubling crystal. This allows the creation of a consistent and accurate frequency axis. After this Lorentzian and Gaussian lineshapes and uncertainties were assigned to the entire spectra. This ultimately led to the assigning of transitions in the range of 664 THz to 676 THz. All code was written by the group and all Mathematica code was written by James Coker.

4.1 Creating Frequency Axis

The IR frequency markers, previously shown, are accurately spaced in frequency due to a GPS disciplined RF source. The IR frequency sweep is not completely linear so that the recorded data is not equally spaced in frequency. An algorithm is employed to identify the large resonance markers so that interpolation may be used to give each measured point the appropriate frequency position. Once this has been done for the up and down portions, they are compared and averaged together to give accurate line intensities and eliminate any frequency bias that may

have existed while the diode laser was sweeping up and down. These $\sim$ 30 GHz sets are then linked together based on their markers and recorded $^{130}Te_2$ lines on either end and ultimately placed in the correct frequency position based on the absolute position of the ^{137}Cs D1 transitions. See Reference A.1.

4.2 Assigning Line Shapes

An interpolation algorithm was used to assign Lorentzian line shapes to all lines in the spectra. Line positions, half-width half-maximums, and uncertainties for all of these were then calculated and recorded. Occasionally a Gaussian profile on either side of an intense line became appropriate, and interpolation was once again used to characterize these profiles. See Reference A.2.

4.3 Assigning Transitions

Once the full line list has been assembled, the process of assigning transition begins. Tellurium alone has all of its protons, electrons, and neutrons paired and is therefore a bosonic atom. It then follows that $^{130}Te_2$ is also a boson and has spin (S) zero (and therefore spin projection along the internuclear axis Σ=0) and is a singlet. Both the BO_u^+ and XO_g^+ are Σ states and therefore have an orbital angular momentum projection along the internuclear axis (Λ) of zero ($\Lambda+\Sigma=\Omega$). *Gerade* states like $X0_g^+$ must have an even orbital angular momentum quantum number (L) and *ungerade* states like $B0_u^+$ must have odd L. The ground state must include a state with L = 0 and is therefore *s*-like.

Evaluating transition probabilities shows that $\Delta L = \pm 1$, $\Delta J = 0, \pm 1$, and $\Delta\Omega = 0$ [Brown and Carrington, 2003, pg. 265]. If $\Omega = 0$, like for our transition, then $\Delta J = \pm 1$ and the excited BO_u^+ state must have L = 1 and is *p*-like. This means that only P ($\Delta J = -1$) and R ($\Delta J = +1$) branches appear for our tran-

sitions; Q branches ($\Delta J = 0$) are forbidden. Given this selection rule for J and knowing that $X0_g^+$ must include the $J = 0$ state, we now know that the BO_u^+ state must include only odd Js beginning with 1 and the XO_g^+ state must include only even Js beginning with 0.

The transition branches can be estimated based on known spectroscopic constants and estimated intensities can be used with a degenerate factor (2J+1) and a Boltzmann factor $exp(E_{Te_2}/kT)$. These can be formed into an image for P and R branches showing roughly where these bandheads begin and end and where they are most intense [Fig. 13, 14]. Note that Franck-Condon factors have not been included and these can change relative intensities by orders of magnitude.

It should be noted that there are other transitions aside from $B0_u^+ \leftarrow X0_g^+$ in our range. These transitions have not been assigned but appear to have Q branch nature. These transitions are likely from the intermediate A1 state which has $\Lambda = \Omega = 1$ and thus only $\Delta J = 0$ is allowed. This state is a triplet and thus has fine structure.

Beginning in a range that the bandhead origin is anticipated to be in, a computer algorithm attempts to fit transition lines based on published constants [Verges et al., 1982] and our energy equation. This is done initially for G_ν and B_ν for low J. These constants are adjusted manually until an accurate fit can be made and then fit by the algorithm for increased accuracy. The constants D_ν and H_ν are then adjusted manually to fit high J values. The lower-order constants are then fit by the algorithm along with the higher-order constants. This is done in an iterative fashion for higher and higher J's until all possible transitions are assigned. See Reference A.4.

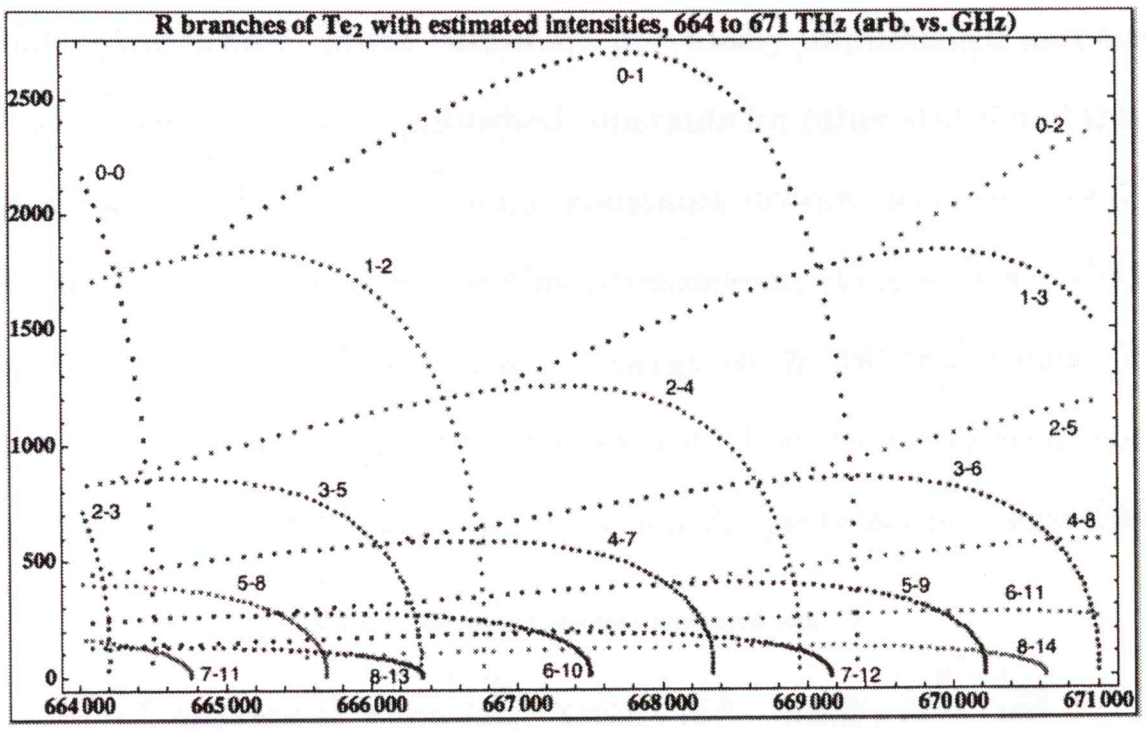

Figure 13: Lower Frequency R Branches

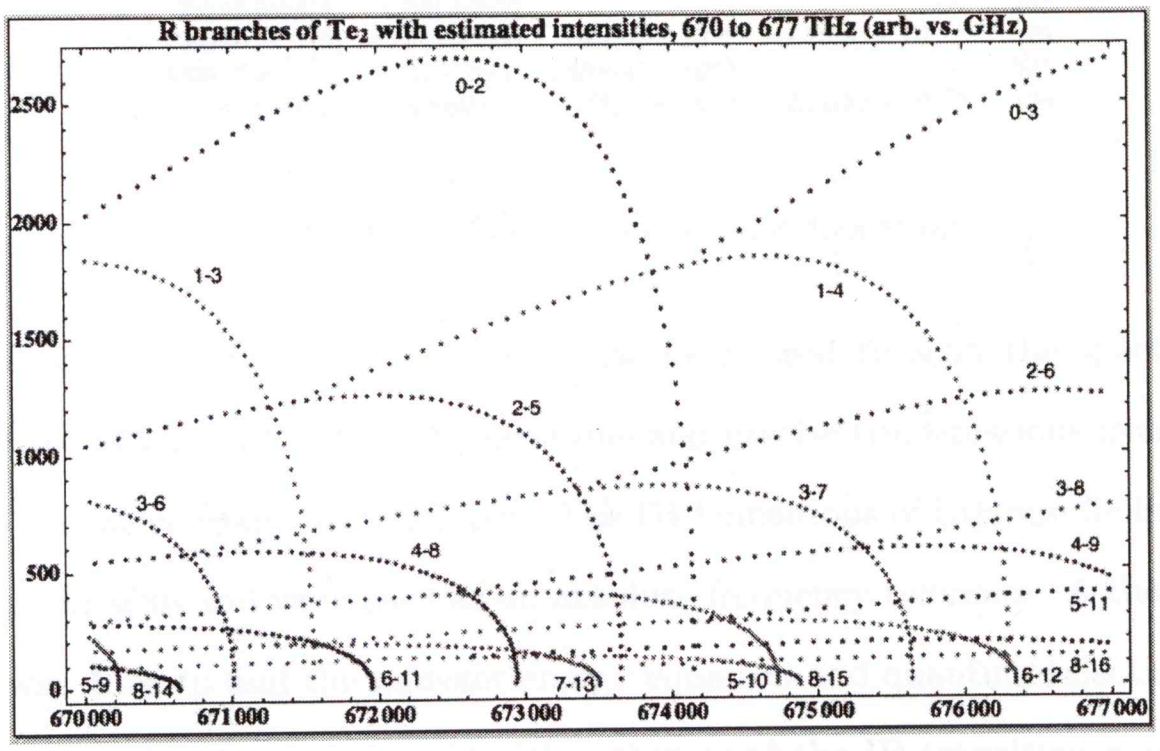

Figure 14: Higher Frequency R Branches

5 Conclusion

Ultimately the $\nu \rightarrow$1-4, 2-5, 3-6, 3-7,5-9, 5-10, 7-11, and 6-12 transitions were identified to high enough J as to yield reliable values for G_ν, B_ν, D_ν, and H_ν [Table 1]. The 5-9 transition was identified but only to high enough J to determine G_ν and B_ν, but the group will determine these constants and other lower frequency

transitions in the future. These values are previously unpublished and are precise enough to be comparable with published constants for other states and transitions. It should be noted that the rotational constants do not decrease monotonically as expected. Others have observed this phenomenon [Verges et al., 1982] and it is due to other states being very close in energy to the B0 transitions. These are presumably the A1 states previously mentioned. The close overlap of these transitions and wavefunctions causes the distortion in spectroscopic constants shown.

TABLE 1. B0 state constants measured (cm^{-1}):

v	T_v	B_v	D_v	H_v	J_{max}
4	22927.2683(5)	0.0319748(2)	$6.29(2) \times 10^{-9}$	$-1.45(6) \times 10^{-14}$	166*
5	23084.4780(1)	0.0318136(1)	$6.67(2) \times 10^{-9}$	$-5.81(7) \times 10^{-14}$	126*
6	23240.29355(3)	0.0316051(1)	$1.247(6) \times 10^{-8}$	$-7.1(1) \times 10^{-13}$	62*
7	23394.6875(4)	0.0316976(4)	$1.57(1) \times 10^{-8}$	$3.23(7) \times 10^{-13}$	104
9	23699.0455(3)	0.031293(2)	—	—	16*
10	23848.9371(3)	0.0310567(9)	$1.09(6) \times 10^{-8}$	$-4.78(9) \times 10^{-12}$	70
11	23997.03615(5)	0.0310778(1)	$1.078(4) \times 10^{-8}$	—	52*
12	24143.8909(1)	0.0308803(1)	$7.36(1) \times 10^{-9}$	$-2.13(5) \times 10^{-14}$	126

Table 1: Determined Spectroscopic Constants

To conclude, a tunable diode laser has been used to scan the spectrum of $^{130}Te_2$ from 664 to 676 THz with the stable and precise transmissions from a FPI used as a relative frequency reference. The D1 transitions of caesium lie in the IR range of our scan and were used as an absolute frequency reference. A theoretical search was done to find the relevant energy equation and quantum selection rules for our molecule. A computer algorithm then used the IR transition markers to create an accurate frequency reference for the entire spectrum. Line shapes were found for the spectrum and transitions for $B0_u^+ \leftarrow X0_g^+$ were assigned to find high order spectroscopic constants.

References

[Allan, 1966] Allan, D. (1966). Statistics of atomic frequency standards. *Proceedings of IEEE*, 54(2):221–230.

[Balasubramanian and Ravimohan, 1987] Balasubramanian, K. and Ravimohan, C. (1987). Theoretical investigation of spectroscopic properties of Te_2. *Journal of Molecular Spectroscopy*, 126:220–230.

[Barrow and du Parcq, 1972] Barrow, R. F. and du Parcq, R. P. (1972). Rotational analysis of the AO_u^+,$BO_u^+ \leftarrow XO_g^+$ systems of gaseous Te_2. *Proceedings of the Royal Society of London A*, 327:279–287.

[Black, 2001] Black, E. D. (2001). An introduction to pound-drever-hall laser frequency stabilization. *Journal of American Physics*, 69(1):79–87.

[Brown and Carrington, 2003] Brown, J. and Carrington, A. (2003). *Rotational Spectroscopy of Diatomic Molecules*. Cambridge Molecular Science.

[Cariou and Luc, 1980] Cariou, J. and Luc, P. (1980). Atlas du spectre d'absorption de la molecule de tellure. Laboratoire Aime, Cotton CNRSII 91405 Orsay, France.

[Courteille et al., 1994] Courteille, P., Ma, L. S., Neuhauser, W., and Blatt, R. (1994). Frequency measurement of $^{130}Te_2$ resonances near 467 nm. *Applied Physics B*, 59:187–193.

[Dunham, 1932] Dunham, J. L. (1932). The energy levels of a rotating vibrator. *Physical Review*, 41:721–731.

[Effantin et al., 1980] Effantin, C., d'Incan, J., Verges, J., Macpherson, M. T., and Barrow, R. F. (1980). A new singlet state of Te_2. *Chemical Physics Letters*, 70(3):560–562.

[Gerginov et al., 2006] Gerginov, V., Calkins, K., Tanner, C. E., McFerran, J. J., Diddams, S., Bartels, A., and Hollberg, L. (2006). Optical frequency measurements of $6s\ ^2S_{1/2}$–$6p\ P_{1/2}$ (D_1) transitions in ^{133}Cs and their impact on the fine-structure constant. *Physical Review A*, 73(032504).

[Gillaspy and Sansonetti, 1991] Gillaspy, J. D. and Sansonetti, C. J. (1991). Absolute wavelength determinations in molecular tellurium: new reference lines for precision laser spectroscopy. *Journal of the Optical Society of America B*, 8(12):2414–2419.

[Gordy and Cook, 1984] Gordy, W. and Cook, R. L. (1984). *Microwave Molecular Spectroscopy*, volume XVIII of *Techniques of Chemistry*. Wiley and Sons, Inc., 3rd edition.

[Jennings et al., 1987] Jennings, D. A., Evenson, K. M., Zink, L. R., Demuynck, C., Destombes, J. L., Lemoine, B., and Johns, J. W. C. (1987). High-resolution spectroscopy of hf from 40 to 1100 cm^{-1}: Highly accurate rotational constants. *Journal of Molecular Spectroscopy*, 2(2):477–480.

[Jha et al., 1969] Jha, B. L., Subbaram, K. V., and Rao, D. R. (1969). Electronic spectra of $^{130}Te_2$ and $^{128}Te_2$. *Journal of Molecular Spectroscopy*, 32:383–397.

[Morse, 1929] Morse, P. M. (1929). Diatomic molecules according to the wave mechanics. ii. vibrational levels. *Physical Review*, 34:57–64.

[Niu et al., 2014] Niu, X., Chen, Q., Zhang, Q., Zhang, H., Chen, J. N. K., Shi, C., and Liu, J. (2014). Using allan variance to analyze the error characteristics of gnss positioning. *GPS Solutions*, 18:231–242.

[Scholl et al., 2005] Scholl, T. J., Rehse, S. J., Holt, R. A., and Rosner, S. D. (2005). Absolute wave-number measurements in $^{130}Te_2$: reference lines span-

ning the 420.0-646.6-nm region. *Journal of the Optical Society of America B*, 22(6):1128–1133.

[Stenholm, 1984] Stenholm, S. (1984). *Foundations of Laser Spectroscopy*. John Wiley and Sons, Inc.

[Stone and Barrow, 1975] Stone, T. J. and Barrow, R. F. (1975). Laser excited fluorescence spectra of gaseous Te_2. *Journal of Canadian Physics*, 53(19):1781–1790.

[Topouzkhanian et al., 1985] Topouzkhanian, A., Babaky, O., Verges, J., Willers, R., and Wellegehausen, B. (1985). Fourier spectroscopic investigations of $^{130}Te_2$ infrared fluorescence and new optically pumped continuous laser lines. *Journal of Molecular Spectroscopy*, 113:39–46.

[Verges et al., 1982] Verges, J., Effantin, C., Babaky, O., d'Incan, J., Prosser, S. J., and Barrow, R. F. (1982). The laser induced fluorescence spectrum of Te_2 studied by fourier transform spectrometry. *Physica Scripta*, 25:338–350.

[Yee and Barrow, 1972] Yee, K. K. and Barrow, R. F. (1972). Observations on the absorption and fluorescence spectra of gaseous Te_2. *Journal of the Chemical Society*, 68:1397–1403.

Appendices

A Mathematica code

A.1 Identifying IR Markers

```
(* global constants *)
path = "/PathName/";
dpath = path <> "data/";
ops = {Joined -> True, Axes -> False, Frame ->
True, PlotRange -> All, ImageSize -> 800,
AspectRatio -> 1/3};
SB = 0.2;
sb = 0.025;
FSR = 0.9990709336; (* from fsrDec13.nb *)
bigN = 337209/FSR;
break = 65550;
\[Gamma]g = 3.;
do7th = 0.318;
blg = 0.265;
Nsets = 126;
allData = Table[0, {i, Nsets}];
(* functions used for fitting *)

L = PDF[CauchyDistribution[xC, \[Gamma]], x];
L5 = a0 (L /. {xC -> x0, \[Gamma] ->
```

```
\[Gamma]0}) +
    a1 (L /. {xC -> x1, \[Gamma] ->
    \[Gamma]1}) + a1 (L /. {xC -> xn1, \[Gamma]
     -> \[Gamma]1}) + a2 (L /. {xC -> x2,
     \[Gamma] -> \[Gamma]2}) + a2 (L /. {xC
     -> xn2, \[Gamma] -> \[Gamma]2});
L7 = L5 + a3 (L /. {xC -> x3, \[Gamma] ->
\[Gamma]3}) + a3 (L /. {xC -> xn3, \[Gamma]
-> \[Gamma]3});
(* major functions *)

getData[name_] := Module[{in, lio, abs, irp, l},
    (* get and parse data, create several
    global arrays *)

    in = Import[name];
    l = Length[in];
    lio = Transpose[in][[1]];
    abs = Transpose[in][[2]];
    irp = Transpose[in][[3]];
    LIu = Take[lio, {1, break}];
    LId = Reverse[Take[lio, {break + 1, l}]];
    ABu = Take[abs, {1, break}];
    ABd = Reverse[Take[abs, {break + 1, l}]];
    IRu = Take[irp, {1, break}];
    IRd = Reverse[Take[irp, {break + 1, l}]];
    Clear[in, lio, abs, irp];
```

```
    ];
truncate[upN_, dnN_] := Module[{},
    (* removes bad edges from data *)
    LIu = Drop[LIu, upN];
    ABu = Drop[ABu, upN];
    IRu = Drop[IRu, upN];
    LId = Drop[LId, dnN];
    ABd = Drop[ABd, dnN];
    IRd = Drop[IRd, dnN];
    ];
patchHole[UD_, fr_, to_, newL_] :=
 Module[{i, out, fill},
    (* unfinished *)
    out = UD;
    For[i = fr, i <= to, i += 1, {
      out[[i]] *= 0;
      }];
    fill = newL - to + fr;
    For[i = to + 1, i <= to + fill, i += 1, {
      out = Insert[out, 0, i];
      }];
    Return[out];
    ];
sampleBreaks[ir_, th_] :=
  Module[{IRs, i, p, thr, swc, left, preFreq,
  f, rInt, minF, maxF, sambks, ti, si},
   (* take IR data and find where sets
```

```
of markers begin/end *)

IRs = {};
ti = 1;
si = ti + 1;
If[Length[th] != 0,
 thr = th[[ti]]; swc = th[[si]];,
 thr = th; swc = -1;
 ];
For[i = 1 + 60, i <= Length[ir] - 60,
i += 1, {p = ir[[i]];
   If[Length[th] != 0 \[And] i == swc,
    ti += 2; si += 2;
    thr = th[[ti]]; If[si <= Length[th],
    swc = th[[si]]](*
    If[
    thr\[Equal]th[[3]], thr=th[[5]],
    thr=th[[3]];
    If[Length[th]>3,swc=th[[4]]];
    ];*)
    ];
   If[p > thr \[And] p == Max[Table[ir[[j]],
   {j, i - 60, i + 60}]],
    AppendTo[IRs, i]];
   }];
left = (IRs[[2]] - IRs[[1]]) < 2000;
preFreq = Table[{0, IRs[[i]]}, {i,
```

```
Length[IRs]}];
f = 0;
For[i = 1, i <= Length[IRs], i += 1, {
  If[left, f += 2 FSR - 2 sb, f += 2 sb];
  preFreq[[i, 1]] += f;
  left = \[Not] left;
  }];
rInt = Interpolation[preFreq];
minF = preFreq[[1, 1]] + sb + FSR/10;
maxF = Last[preFreq][[1]];
sambks = Table[ff, {ff, minF - 2 FSR,
maxF + 2 FSR, FSR/5}];
sambks = Quiet[Floor[rInt[sambks]]];
  While[sambks[[1]] < 0, sambks =
  Drop[sambks, 1]];
  While[Last[sambks] > Length[ir],
  sambks = Drop[sambks, -1]];
  Return[sambks];
  ];
viewable1D[dat_, length_, filler_, points_] :=
Module[{out, i},
  (* take 1 1D array and add filler to make
  it usable for \
Manipulate[] *)
  out = Table[filler, {i, length}];
  For[i = 1, i <= Length[dat], i += 1, {
    out[[dat[[i]]]] += points;
```

```
    }];
  Return[out];
  ];
XaxisInterp[ir_, breaks_, brst_, brstp_, n_, m_]
:= Module[{
   (* finds the interpolation function from
   index to frequency *)

    marks, num, f, t, x5, x7, sample, pM,
    pars5, pars7, set, \[Delta], xg, fifth,
    nlmf, pars, i2f, out, nn, mm
   },
  marks = {};
  nn = n;
  mm = m;
  For[num = brst, num < Length[breaks] + brstp,
  num += 1, {
    f = breaks[[num]];
    t = breaks[[num + 1]];
    Clear[xn3, xn2, xn1, x0, x1, x2, x3,
     x, \[Gamma]0, \[Gamma]1, \[Gamma]2,
     \[Gamma]3, a0, a1, a2, a3, bl, pars5,
     pars7];
    x5 = {xn2, xn1, x0, x1, x2} - 1 + f;
    x7 = Join[{xn3}, x5, {x3}] - 1 + f;
    sample = Take[ir, {f, t}];
    pM = Position[sample, Max[sample]]
```

```
[[1, 1]]; set = If[Max[sample] > do7th,
{L7, pars7, x7, 3}, {L5, pars5, x5, 2}];
\[Delta] = (t - f)/8;
xg = -f + Table[f + i \[Delta], {i,
1., 7.}];
fifth = Abs[xg[[3]] - pM] > Abs[xg[[5]]
- pM];
xg += pM - If[fifth, xg[[5]], xg[[3]]];
pars5 = {{bl, blg}, a0, {x0, xg[[4]]},
{\[Gamma]0, \[Gamma]g},
  a1, {x1, xg[[5]]}, {\[Gamma]1, \[Gamma]g},
  {xn1, xg[[3]]}, a2, {x2, xg[[6]]},
  {\[Gamma]2, \[Gamma]g}, {xn2, xg[[2]]}};
pars7 =
 Join[pars5, {a3, {x3, xg[[7]]}, {\[Gamma]3,
 \[Gamma]g}, {xn3, xg[[1]]}}];
nlmf = NonlinearModelFit[sample, bl +
set[[1]],
set[[2]], x];
pars = nlmf["BestFitParameters"];
If[Max[sample] > do7th \[And] Abs[(xn3 /.
pars) -
xg[[1]]] < 10,
 AppendTo[marks, {(-1 + f + xn3) /. pars,
 nn,
  mm, -3}]];
If[Abs[(xn2 /. pars) - xg[[2]]] < 10,
```

```
 AppendTo[marks, {(-1 + f + xn2) /. pars,
 nn,
 mm, -2}]];
If[Abs[(xn1 /. pars) - xg[[3]]] < 10,
 AppendTo[marks, {(-1 + f + xn1) /. pars,
 nn,
 mm, -1}]];
If[Abs[(x0 /. pars) - xg[[4]]] < 10,
 AppendTo[marks, {(-1 + f + x0) /. pars,
 nn, mm, 0}]];
If[Abs[(x1 /. pars) - xg[[5]]] < 10,
 AppendTo[marks, {(-1 + f + x1) /. pars,
 nn, mm, 1}]];
If[Abs[(x2 /. pars) - xg[[6]]] < 10,
 AppendTo[marks, {(-1 + f + x2) /. pars,
 nn, mm, 2}]];
 If[Max[sample] > do7th \[And] Abs[(x3 /.
 pars) -
 xg[[7]]] < 10,
  AppendTo[marks, {(-1 + f + x3) /. pars,
  nn, mm, 3}]];
 If[mm == 2, mm = -2; nn += 1;, mm += 1];
 }];
i2f = Table[{marks[[i, 1]],
  FSR marks[[i, 2]] + SB marks[[i, 3]] +
  sb marks[[i, 4]]}, {i,
  Length[marks]}];
```

```
    out = Interpolation[i2f];
    (*Print[Last[i2f]];*)
    Return[out];
    ];
toFreq[intFun_, data_] := Module[{out},
    (* puts frequency x-axis on data *)

    out = Quiet[Table[{intFun[i], data[[i]]},
    {i, 1,
    Length[data]}]];
    Return[out];
    ];
avgPlus[fdat1_, ft1_, fdat2_, ft2_, fdat3_: {},
 ft3_:
{}] := Module[{
    mMHz, MMHz, out, inter1, inter2, inter3, i,
    f, n,
    outU, outD,
    out3, boo3},
    (* averages 2 data sets, returns all 3 with
    same x-axis *)

    mMHz = 1000 Min[Join[ft1, ft2, ft3]];
    MMHz = 1000 Max[Join[ft1, ft2, ft3]];
    out = Table[{i/1000., 0}, {i, Floor[mMHz],
    Ceiling[MMHz]}];
    inter1 = Interpolation[fdat1];
```

```
inter2 = Interpolation[fdat2];
outU = Table[{out[[i, 1]], -inter1[out[[i,
1]]]},
{i, Length[out]}];
outD = Table[{out[[i, 1]], -inter2[out[[i,
1]]]},
{i, Length[out]}];
If[Length[fdat3] > 10,
 inter3 = Interpolation[fdat3];
 out3 =
  Table[{out[[i, 1]], -inter3[out[[i, 1]]]},
  {i, Length[out]}];
 ];
boo3 = Length[ft3] > 1;
For[i = 1, i <= Length[out], i += 1, {
  f = out[[i, 1]];
  n = 0;
  If[f >= ft1[[1]] \[And] f <= ft1[[2]], n +=
   1; out[[i, 2]] += inter1[f]];
  If[f >= ft2[[1]] \[And] f <= ft2[[2]], n +=
   1; out[[i, 2]] += inter2[f]];
  If[boo3 \[And] f >= ft3[[1]] \[And] f <=
  ft3[[2]],
  n += 1;
   out[[i, 2]] += inter3[f]];
  If[n != 0, out[[i, 2]] /= n, Print[f]];
  }];
```

```
    If[boo3, out = {out, outU, outD, out3}, out =
    {out, outU, outD}];
    Return[out];
    ];

.....

    (* view the raw data *)
getData[dpath <> "13.02.08.tsv"];
truncate[1, 1];(* up beginning, down begining *)

truncate[-1, -1];(* up end, down end *)
ListPlot[{LIu, -3 +
    ABu/2., 0.7 - 5 IRu}, ops]
ListPlot[{LId, -3 + ABd/2., 0.7 - 5 IRd}, ops]
ListPlot[{IRu, 0.5 - IRd}, ops]

.....

sambks = sampleBreaks[
    IRu, {0.14, 38000 - 1050, 0.13, 60500 -
    1050, 0.126}];
sambksV = viewable1D[sambks, Length[IRu], 0, 0.4];
sambks2 =
  sampleBreaks[
    IRd, {0.138, 12500, 0.128, 28700, 0.12, 37000,
    0.11, 37400, 0.4,
```

```
    41300, 0.11, 41700, 0.4, 45700, 0.122, 60000,
    0.128}];
sambksV2 = viewable1D[sambks2, Length[IRd], 0,
0.4]; w = 4000;
Manipulate[
 ListPlot[{Take[IRu, {m, m + w}], Take[sambksV,
 {m, m + w}]},
  PlotRange -> {0.09, 0.14}, ops],
 {m, 1, Length[IRu] - w, Floor[0.8 w]}]
Manipulate[
 ListPlot[{Take[IRd, {m, m + w}], Take[sambksV2,
 {m, m + w}]},
  PlotRange -> {0.09, 0.14}, ops],
 {m, 1, Length[IRd] - w, Floor[0.8 w]}]
```

.....

```
int = XaxisInterp[IRu, sambks, 1, 0, bigN - 2938
- 1 + 4, 2];LIu\[Nu] = toFreq[int, LIu];
int2 = XaxisInterp[IRd, sambks2, 1, 0, bigN -
2938 - 1 + 4, 2];
LId\[Nu] = toFreq[int2, LId];
ListPlot[LIu\[Nu], ops]
ListPlot[LId\[Nu], ops]
```

.....

```
dat = avgPlus[LIu\[Nu], {334274.3 - 1 + 4,
334303.5 -
1 + 4},
    LId\[Nu], {334274.3 - 1 + 4, 334295 - 1 + 4}];
w = 4000;
Manipulate[
 ListPlot[{Take[dat[[1]], {m, m + w}],
 Take[dat[[2]],   {m, m + w}],
    Take[dat[[3]], {m, m + w}]}, PlotRange ->
    {-1, 1.5}, ops],
 {m, 1, Length[dat[[1]]] - w, Floor[0.8 w]}]


.........

allData[[1]] = dat[[1]];

.........

Export[path <> "everything.csv", allData]
```

A.2 Verifying Scans and Averaging

```
path = "YourPathName";
ops = {Joined -> True, Frame -> True, PlotRange
-> All, Axes -> False,
     ImageSize -> 700};
all = ToExpression[Import[path <>
```

```
"YourDataImportFile.type"]];
all = Sort[all, #1[[1, 1]] < #2[[1, 1]] &];
all[[110]] = Take[all[[110]], 26800];
lookAtTwo[one_, two_, ii_] :=
  Module[{M1, m2, window, i, j, ONE, TWO},
   M1 = Last[one][[1]];
   m2 = two[[1, 1]];
   window = {m2 - 0.1, M1 + 0.1};
   i = 1;
   While[i < Length[one] \[And] one[[i, 1]] <
   window[[1]], i += 1];
   j = i;
   While[j < Length[one] \[And] one[[j, 1]] <
   window[[2]], j += 1];
   j -= 1;
   ONE = Take[one, {i, j}];
   i = 1;
   While[i < Length[two] \[And] two[[i, 1]] <
   window[[1]], i += 1];
   j = i;
   While[j < Length[two] \[And] two[[j, 1]] <
   window[[2]], j += 1];
   j -= 1;
   TWO = Take[two, {i, j}];
   (*For[i=1,i\[LessEqual]Length[TWO],i+=1,
   TWO[[i,2]]*=-1];*)
```

```
    Print["Now comparing " <> ToString[ii] <> "
    and " <>
      ToString[ii + 1]];
    Print[ListPlot[{ONE, TWO}, AspectRatio -> 1/4,
    ImageSize -> 1000,
      ops]];
    ];

 ..........

m = all[[1, 1, 1]];
M = Last[Last[all]][[1]];
avg = Table[{f, 0, 0}, {f, m, M, 0.001}];
la = Length[all];
lav = Length[avg];
Monitor[
 For[i = 1, i <= la, i += 1, {
   temp = all[[i]];
   stF = temp[[1, 1]];
   p = Round[1000 (stF - m) + 1];
   lt = Length[temp];
   If[Length[p] > 0, Print[Length[p], " ", i]];
   addTo = Take[avg, {p, p + lt - 1}];
   av = Mean[Drop[Transpose[temp], 1][[1]]];
   If[av > 0, \[CapitalPi] = 1, \[CapitalPi] =
   -1]; adder = Table[{0, \[CapitalPi] temp[[j,
   2]], 1}
```

```
  , {j, lt}];
  addTo += adder;
  avg = Join[Take[avg, {1, p - 1}], addTo,
    Take[avg, {p + lt, lav}]];
  }];
For[i = 1, i <= lav, i += 1, {
  If[avg[[i, 3]] != 0,
    avg[[i, 2]] /= avg[[i, 3]]
    ];
  }];
avg = Transpose[Drop[Transpose[avg], -1]];,
i]
```

. . . . . .

```
Export[path <> "YourAveragedDataExportFile.type",
avg]
```

A.3 Assigning Line Shapes

```
path = "/YourPath/";
ops = {Joined -> True, PlotRange -> All, Frame
-> True,
    Axes -> False,
        ImageSize -> 700};
FSR = 0.9990709336; (* from fsrDec13.nb *)
bigN = 337209/FSR;
```

```
os = 335120.5627597 - .847681 - SetPrecision[FSR
(bigN -
2092), 9];
(* marker number found in te2jeffpkg.nb,
335121 GHz is Cs line #3 from Tanner,
848 MHz number from Cs #3 HeNe zero measurement *)

dat = ToExpression[Import[path <>
"YourAveragedDataFile.type"]][[1]];
dat += os Table[{1, 0}, {i, Length[dat]}];
L = PDF[CauchyDistribution[x0, \[Gamma]], x];
G = PDF[NormalDistribution[x0, \[Gamma]], x];
window[d_, fr_, to_] := Module[{first, last,
step,
i, j, out},
        first = dat[[1, 1]];
        last = Last[dat][[1]];
        step = dat[[2, 1]] - dat[[1, 1]];
        i = Floor[1 + (fr - first)/step];
        j = i + Floor[(to - fr)/step];
        If[i < 1,
          i = 1;
          minus = 1000 Floor[first/1000.];,
          minus = 1000 Floor[fr/1000.];
          ];
        If[j > Length[d], j = Length[d]];
        out = Take[d, {i, j}];
```

```
        out -= minus Table[{1, 0}, {i,
        Length[out]}];
        Return[out];
        ];
autoFit[samp_, th_, doingFits_] :=
    Module[{out, Ysamp, hw, i, ys, local},
      out = {};
      Ysamp = Transpose[samp][[2]];
      hw = 20;
      For[i = 1 + hw, i <= Length[Ysamp] - hw,
      i += 1,
      {
        ys = Ysamp[[i]];
        local = Take[Ysamp, {i - hw, i + hw}];

If[ys == Max[local] \[And] ys > th,
AppendTo[out,
samp[[i]]]];
      }];
 If[\[Not] doingFits,
   If[Length[out] < 1, Print[ListPlot[samp,
   ops]],
     Print[
       ListPlot[{samp, out}, Joined ->
       {True, False},
         PlotStyle -> {Thin, Red}, ops]];
     Print[Transpose[out][[1]]];
```

```
        ]];
      out = Transpose[out][[1]];
      Return[out];
      ];
multiFit[samp_, ags_, del_, xgs_, ggss_,
doingFits_] := Module[{fun, i, is, str, pars,
nlmf, eq, out, rems,
    gss, er},
      rems = Table[{del[[i]]}, {i, Length[del]}];
      gss = Delete[ags, rems];
      If[Length[xgs] > 0, gss = Join[gss, xgs]];
      If[\[Not] doingFits, out = 0,
        fun = bl + a1 (L /. {x0 -> x01, \[Gamma]
        ->
        \[Gamma]1});
        pars = {{bl, 0}, {a1, 0.002}, {x01,
        gss[[1]]},
        {\[Gamma]1,
      0.004}};
        out = "";
        For[i = 2, i <= Length[gss], i += 1, {
          is = ToString[i];
          str =
            "a" <> is <> "*(L/.{x0\[Rule]x0"
              <> is <>
               ",\[Gamma]\[Rule]\[Gamma]"
              <> is <> "})";
```

```
    fun += ToExpression[str];
    str =
      "{{a" <> is <> ",0.002},{x0" <>
      is <> "," <>
        ToString[gss[[i]]] <> "},
        {\[Gamma]" <> is <>
",0.004}}";
    pars = Join[pars, ToExpression[str]];
    }];
For[i = 1, i <= Length[ggss], i += 1, {
    is = ToString[i];
    str =
      "ag" <> is <> "*(G/.{x0\[Rule]x0g"
       <> is <>
        ",\[Gamma]\[Rule]\[Gamma]g"
        <> is <> "})";
    fun += ToExpression[str];
    str =
      "{{ag" <> is <> ",0.02},{x0g" <>
      is <> "," <>
        ToString[ggss[[i]]] <> "},
        {\[Gamma]g" <>
        is <>
",0.002}}";
    pars = Join[pars, ToExpression[str]];
    }];
nlmf = NonlinearModelFit[samp, fun,
```

```
    pars, x];
    eq = nlmf["BestFit"];
    bfp = nlmf["BestFitParameters"]; (*
must remain global! *)
    pe = nlmf["ParameterErrors"]; (*
must remain global! *)
    Print[Show[
        ListPlot[samp, Joined -> False, ops],
        Plot[eq, {x, First[samp][[1]],
        Last[samp][[1]]},
          PlotRange -> All, PlotStyle -> Red]
        ]];
    For[i = 1, i <= Length[gss], i += 1, {
    is = ToString[i];
    out = out <> "
        ";
    out = out <>
        ToString[

SetPrecision[ToExpression["minus+(x0" <>
is <>
"/.bfp)"],
            12]] <> "," <>
ToString[ToExpression["pe[[" <>
 ToString[3 i]
<> "]]"]] <>
    "," <>
```

```
ToString[ToExpression["(\[Gamma]" <> is
<> "/.bfp)"]] <> "," <>
ToString[
 ToExpression[
  "pe[[" <> ToString[3 i + 1] <> "]]"]]
  <>"," <>

ToString[ToExpression["(a" <> is <>
"/.bfp)"]] <>
"," <>

ToString[
 ToExpression[
  "pe[[" <> ToString[3 i - 1] <> "]]"]]
  <>
"," <> "L";
    }];
For[i = 1, i <= Length[ggss], i += 1, {
    is = ToString[i];
    out = out <> "
        ";
    out = out <>
        ToString[

 SetPrecision[ToExpression["minus+(x0g"
 <> is <>
 "/.bfp)"],
```

```
12]] <> "," <>

ToString[ToExpression["pe[[" <>
ToString[3  i] <>
"]]"]] <>
        "," <>

ToString[ToExpression["(\[Gamma]g"
 <> is <>
"/.bfp)"]] <>
        "," <>

ToString[
 ToExpression[
  "pe[[" <> ToString[3  i + 1] <>
  "]]"]] <>

"," <>

ToString[ToExpression["(ag" <> is <>
"/.bfp)"]] <>
"," <>

ToString[
 ToExpression[
  "pe[[" <> ToString[3  i - 1] <>
  "]]"]] <>
```

```
","  <>  "G";
      }];
Print[
  ToString[Length[gss]] <> " lorentzian
  fits and " <>
    ToString[Length[ggss]] <> "
    gaussian fits"];
For[i = 1, 3 i <= Length[pe], i += 1, {
    er = pe[[3  i]];
    str = ToString[bfp[[3  i]]];

If[er >= 0.001 \[And] StringDrop[
StringTake[str , 3], 2]
!= "g",
        Print[
          "Line " <> str <> " has
          uncertainty " <>
            ToString[NumberForm[
            SetPrecision[1000 er,
              2]]] <>
   " MHz"]
          ]
       }];
  ];
Return[out];
];
```

```
wbut = Button["Write to file", {
        s = OpenAppend[path <>
        "YourLineList.csv"];
        WriteString[s, write];
        Close[s];
        sr2 = Import[path <>
        "YourLineList.csv"];
        lastLine = SetPrecision[
        Last[sr2][[1]], 9];
        tot = ToString[Length[sr2]]
        <> " lines total";
        }];
```

.....

```
ButtonBar[{"Do Fits" :> (doFits = True),
    "Just Look" :> (doFits = False)}]
Dynamic[doFits]
wbut
Dynamic[lastLine]
Dynamic[tot]
```

.....

```
set = 610;
set2 = 334000;
set3 = 334005;
```

```
piece = window[dat, set + set2, set + set3];
gs = autoFit[piece, 0.035, doFits];
removes =
  0;(* must use {} if removing lines, must
  NOT use {} if not removing \
lines *)
moreGuesses = 0; (* enter frequency, GHz *)

gaussGuesses = 0;
write = multiFit[piece, gs, removes, moreGuesses,
gaussGuesses,
      doFits];
```

A.4 Spectroscopy

```
url = "URL_Linelist";
path = "YourPath";
ops = {Joined -> True, PlotRange -> All, Frame ->
True, Axes -> False,
     ImageSize -> 700};
list = Import[url];
list = Sort[Drop[list, 1]];
labList = Import[path <> "labeled2.csv"];
listNG = list;
i = 1;
While[i <= Length[listNG],
  If[listNG[[i, 7]] == "G", listNG =
```

```
  Delete[listNG, i],
   i += 1]];
listNG = Table[{listNG[[i, 1]], listNG[[i, 3]],
listNG[[i, 5]], 0, 0,
    0, 0}, {i, Length[listNG]}];
L = PDF[CauchyDistribution[x0, \[Gamma]], x];
m = 335090.97147179116;
M = 338203.77147179114;
Tc = 650;
kT = 0.69503568 (273.15 + Tc);
c30 = 29.9792458;
totalMax = 338205;
window[fr_, to_, sc_, useSep_] :=
  Module[{beg, end, i, j, listO, listPiece, fun,
list2, xs, xc, hw,
 ys, out},
beg = If[fr < m, m, fr];
end = If[to > M, M, to];
beg -= 1;
end += 1;
If[useSep,
 listO =
  Table[{sepped[[2, i, 1]], 0, sepped[[2,
  i, 2]], 0,
    sepped[[2, i, 3]], 0, "L"}, {i,
     Length[sepped[[2]]]}],
 listO = list;
```

```
 ];
i = 1;
While[i <= Length[listO] \[And] listO[[i, 1]]
<
 beg, i += 1];
j = i;
While[j <= Length[listO] \[And] listO[[j, 1]]
<
end, j += 1];
j -= 1;
listPiece = Take[listO, {i, j}];
i = 1;
While[i <= Length[listPiece],
 If[listPiece[[i, 7]] == "G", listPiece =
  Delete[listPiece, i],
  i += 1]
 ];
fun = 0;
For[i = 1, i <= Length[listPiece], i += 1, {
  fun +=
    listPiece[[i,
      5]] (L /. {x0 -> listPiece[[i, 1]],
      \[Gamma] ->
        listPiece[[i, 3]]});
  }];
list2 = listO;
i = 1;
```

```
While[i <= Length[list2],
 If[list2[[i, 7]] == "G", list2 =
 Delete[list2, i],
  i += 1]];
i = 1;
While[i <= Length[list2] \[And] list2[[i, 1]]
< beg
 - 1, i += 1];
j = i;
While[j <= Length[list2] \[And] list2[[j, 1]]
< end
 + 1, j += 1];
j -= 1;
list2 = Take[list2, {i, j}];
xs = {};
For[i = 1, i <= Length[list2], i += 1, {
  xc = list2[[i, 1]];
  hw = list2[[i, 3]];
  xs = Join[xs, Table[xc + j hw, {j, -3, 3,
  1}]];
  }];
xs = Join[xs, Table[k, {k, beg, end, 0.1}]];
xs = Sort[xs];
ys = fun /. x -> xs;
out = Transpose[{xs, sc ys}];
Return[out];
];
```

```
cons = Import[path <> "Te2cons.csv"];
U[v_, J_] :=
  Te + G[v] + B[v] J (J + 1) - Dv[v] J^2
  (J + 1)^2 +
   H[v] J^3 (J + 1)^3;
G[V_] := \[Omega] (V + 1/2) - \[Omega]x (V +
1/2)^2 +
\[Omega]y (V +
      1/2)^3 + \[Omega]z1 (V + 1/2)^4 +
      \[Omega]z2
       (V + 1/
      2)^5 + \[Omega]z3 (V + 1/2)^6 + \[Omega]z4
      (V + 1/
      2)^7 + \[Omega]z5 (V + 1/2)^8;
B[V_] := Be - \[Alpha] (V + 1/2) + \[Gamma]1
(V + 1/
      2)^2 + \[Gamma]2 (V + 1/2)^3 + \[Gamma]3
      (V + 1/
      2)^4 + \[Gamma]4 (V + 1/2)^5 + \[Gamma]5
      (V + 1/2)^6;
Dv[V_] :=
  De + \[Beta]1 (V + 1/2) + \[Beta]2 (V + 1/2)^2
   +
   \[Beta]3 (V + 1/
      2)^3;
H[V_] := He + g1 (V + 1/2) + g2 (V + 1/2)^2;
sub[state_] := Module[{col, pcol, out},
```

```
col = Switch[state, "X0", 2, "X1", 4, "B0", 6,
 "B0C", 8];
pcol = col + 1;
out = {
  Te -> cons[[2, col]]*10^cons[[2, pcol]],
  \[Omega] -> cons[[3, col]]*10^
  cons[[3, pcol]],
  \[Omega]x -> cons[[4, col]]*10^
  cons[[4, pcol]],
  \[Omega]y -> cons[[5, col]]*10^
  cons[[5, pcol]],
  \[Omega]z1 -> cons[[6, col]]*10^
  cons[[6, pcol]],
  \[Omega]z2 -> cons[[7, col]]*10^
  cons[[7, pcol]],
  \[Omega]z3 -> cons[[8, col]]*10^
  cons[[8, pcol]],
  \[Omega]z4 -> cons[[9, col]]*10^
  cons[[9, pcol]],
  \[Omega]z5 -> cons[[10, col]]*10^
  cons[[10, pcol]],
  Be -> cons[[11, col]]*10^cons[[11, pcol]],
  \[Alpha] -> cons[[12, col]]*10^cons[[12,
  pcol]],
  \[Gamma]1 -> cons[[13, col]]*10^cons[[13,
  pcol]],
  \[Gamma]2 -> cons[[14, col]]*10^cons[[14,
```

```
pcol]],
\[Gamma]3 -> cons[[15, col]]*10^cons[[15,
pcol]],
\[Gamma]4 -> cons[[16, col]]*10^cons[[16,
pcol]],
\[Gamma]5 -> cons[[17, col]]*10^cons[[17,
pcol]],
De -> cons[[18, col]]*10^cons[[18, pcol]],
\[Beta]1 -> cons[[19, col]]*10^cons[[19,
pcol]],
\[Beta]2 -> cons[[20, col]]*10^cons[[20,
pcol]],
\[Beta]3 -> cons[[21, col]]*10^cons[[21,
pcol]],
He -> cons[[22, col]]*10^cons[[22, pcol]],
g1 -> cons[[23, col]]*10^cons[[23, pcol]],
g2 -> cons[[24, col]]*10^cons[[24, pcol]]
};
Return[out];
];
X0 = sub["X0"];
X1 = sub["X1"];
B0 = sub["B0"];
VAR = {Te ->
Te, \[Omega] -> \[Omega], \[Omega]x ->
\[Omega]x,
\[Omega]y -> \
```

```
\[Omega]y, \[Omega]z1 -> \[Omega]z1, \[Omega]z2
->
\[Omega]z2, \
\[Omega]z3 -> \[Omega]z3, \[Omega]z4 ->
\[Omega]z4,
\[Omega]z5 -> \
\[Omega]z5,
    Be -> Be, \[Alpha] -> \[Alpha], \[Gamma]1 ->
    \[Gamma]1, \[Gamma]2 \
-> \[Gamma]2, \[Gamma]3 -> \[Gamma]3, \[Gamma]4
-> \[Gamma]4, \
\[Gamma]5 -> \[Gamma]5,
    De -> De, \[Beta]1 -> \[Beta]1, \[Beta]2 ->
    \[Beta]2, \[Beta]3 -> \
\[Beta]3, He -> He, g1 -> g1, g2 -> g2};
B0C = sub["B0C"];
branchList[gS_, eS_, Vg_, Ve_, Jm_, JM_, br_] :=
  Module[{low, high, out, j, jj, en, mb, Jint},
   low = U[Vg, jj] /. gS;
   high = U[Ve, jj + br] /. eS;
   Jint = 2;
   out = Table[{0, 0}, {i, Jm, JM, Jint}];
   j = 1;
   For[jj = Jm, jj <= JM, jj += Jint, {
     en = high - low;
     mb = (2 jj + 1) Exp[-low/kT];
     out[[j]] += {en, -mb};
```

```
      j += 1;
      }];
    Return[out];
    ];
makeBases[v_] := Module[{Tbase, Gbase, Bbase,
Dbase,
Hbase, out},
    Tbase = Te /. B0;
    Gbase = G[v] /. B0;
    Bbase = B[v] /. B0;
    Dbase = Dv[v] /. B0;
    Hbase = H[v] /. B0;
    out = {Tbase, Gbase, Bbase, Dbase, Hbase};
    Return[out];
    ];
makeSim[bss_, \[Delta]s_, vg_, ve_] :=
Module[{Sb, bl,
 out},
   Sb = Join[
     {Te -> bss[[1]] + bss[[2]] + \[Delta]s[[1]],
      Be -> bss[[3]] + \[Delta]s[[2]],
      De -> bss[[4]] + \[Delta]s[[3]], \[Omega]
      -> 0,
       \[Omega]x ->
       0, \[Omega]y -> 0, \[Alpha] -> 0,
      He -> bss[[5]] + \[Delta]s[[4]]},
     B0
```

```
  ];
bl = c30  0.5  Join[branchList[X0, Sb, vg, ve,
 2,
250, 1],

    branchList[X0, Sb, vg, ve, 2, 250, -1]];
bl = Sort[bl];
While[bl[[1, 1]] < min, bl = Drop[bl, 1]];
While[Last[bl][[1]] > max, bl = Drop[bl, -1]];
out = Table[{{bl[[i, 1]] - 0.01, 0},
    bl[[i]], {bl[[i, 1]] + 0.01, 0}}, {i,
    Length[bl]}];
out = Flatten[out, 1];
    Return[out];
    ];
autoAssigner[lass_, params_, vx_, vb_, loLimit_]
:=  Module[{subs, band, form, xlng, listodiffs,
pos, out,  i, jMp, jMr,
     jt, br},
    subs =
     Join[params, {g1 -> 0,
       g2 -> 0, \[Beta]1 -> 0, \[Beta]2 -> 0,
       \[Beta]3 ->
        0, \[Alpha] -> 0, \[Gamma]1 -> 0,
        \[Gamma]2 -> 0,
        \[Gamma]3 ->
        0, \[Gamma]4 -> 0, \[Gamma]5 -> 0,
```

```
    \[Omega] -> 0,
    \[Omega]x ->
    0, \[Omega]y -> 0, \[Omega]z1 -> 0,
    \[Omega]z2 ->
    0, \[Omega]z3 -> 0, \[Omega]z4 -> 0,
    \[Omega]z5 ->
    0}];
Clear[jx, jb];
form = ((U[vb, jb] /. subs) - (U[vx, jx] /.
X0));
band =
 Sort[Join[
   Table[{(0.5 c30 form /. {jx -> j, jb ->
    j + 1}), j,
     1}, {j, 0,
      250, 2}],
   Table[{(0.5 c30 form /. {jx -> j, jb ->
     j - 1}), j,
    -1}, {j, 2,
      250, 2}]]];
Print[Length[band]];
While[band[[1, 1]] < loLimit, band =
 Drop[band, 1]];
While[Last[band][[1]] > totalMax, band =
Drop[band,
  -1]];
Print[band];
```

```
jMp = 0;
jMr = 0;
For[i = 1, i <= Length[band], i += 1, {
  jt = band[[i, 2]];
  br = band[[i, 3]];
  If[br == 1,
   If[jt > jMr, jMr = jt],
   If[jt > jMp, jMp = jt]
   ];
  }];
Print["P branch max J: " <> ToString[jMp]];
Print["R branch max J: " <> ToString[jMr]];
xlng = Transpose[lass][[1]];
out = lass;
For[i = 1, i <= Length[band], i += 1, {
  listodiffs = Abs[band[[i, 1]] - xlng];
  pos = Position[listodiffs, Min[listodiffs]]
  [[1, 1]];
  If[out[[pos, 7]] != 0,
   Print[ToString[band[[i, 1]]] <> " tried to
   match
   twice"],
   out[[pos]] += {0, 0, 0, vx, vb,
   band[[i, 2]],
   band[[i, 3]]}];
  }];
Return[out];
```

```
    ];
separator[asdList_, vx_, vb_] := Module[{i, mvs,
out1, out2},
    mvs = {};
    For[i = 1, i <= Length[asdList], i += 1, {
      If[asdList[[i, 4 ;; 5]] != {vx, vb},
      AppendTo[mvs, i]];
      }];
    out2 = {};
    For[i = 1, i <= Length[mvs], i += 1, {
      AppendTo[out2, asdList[[mvs[[i]]]]];
      }];
    mvs = Table[{mvs[[i]]}, {i, Length[mvs]}];
    out1 = Delete[asdList, mvs];
    out1 = Transpose[Drop[Transpose[out1], -4]];
    out2 = Transpose[Drop[Transpose[out2], -4]];
    Return[{out1, out2}]
    ];
plotSeparated[sepd_, fr_, to_, opts_] :=
  Module[{i, j, k, fun1, fun2, subs},
    fun1 = 0;
    fun2 = 0;
    j = 1;
    While[j <= Length[sepd[[2]]] \[And] fr >
    sepd[[2, j, 1]] + 2,
     j += 1];
    k = j;
```

```
While[k <= Length[sepd[[2]]] \[And] to >
sepd[[2, j, 1]] - 2,
 k += 1];
k -= 1;

For[i = j, i <= k, i += 1, {
  subs = sepd[[2, i, 1 ;; 3]];
  fun2 += (subs[[3]] L /. {x0 -> subs[[1]],
  \[Gamma] -> subs[[2]]});
  }];

For[i = 1, i <= Length[sepd[[1]]], i += 1, {
  subs = sepd[[1, i, 1 ;; 3]];
  fun1 += (subs[[3]] L /. {x0 -> subs[[1]],
  \[Gamma] -> subs[[2]]});
  }];
 Return[Plot[{fun1, fun2}, {x, fr, to}, opts]];
 ];
makeAttempt[params_, vx_, vb_, loLimit_, sc_] :=
 Module[{subs, form, out},
  subs =
   Join[params, {g1 -> 0,
     g2 -> 0, \[Beta]1 -> 0, \[Beta]2 -> 0,
     \[Beta]3 ->
      0, \[Alpha] -> 0, \[Gamma]1 -> 0,
      \[Gamma]2
      -> 0, \[Gamma]3 ->
```

```
    0, \[Gamma]4 -> 0, \[Gamma]5 -> 0,
    \[Omega]
    -> 0, \[Omega]x ->
    0, \[Omega]y -> 0, \[Omega]z1 -> 0,
     \[Omega]z2
    ->
    0, \[Omega]z3 -> 0, \[Omega]z4 -> 0,
    \[Omega]z5
    -> 0}];
Clear[jx, jb];
form = ((U[vb, jb] /. subs) - (U[vx, jx] /.
X0));
out = Sort[Join[
Table[{(0.5 c30 form /. {jx -> j, jb ->
j + 1}),
 sc}, {j, 2,
  200, 2}],
Table[{(0.5 c30 form /. {jx -> j, jb ->
j - 1}),
 sc}, {j, 2,
  200, 2}],
Table[{(0.01 + 0.5 c30 form /. {jx -> j,
 jb ->
j + 1}), 0}, {j,
  2, 200, 2}],
Table[{(0.01 + 0.5 c30 form /. {jx -> j,
jb ->
```

```
    j - 1}), 0}, {j,
      2, 200, 2}],
    Table[{(-0.01 + 0.5 c30 form /. {jx -> j,
    jb ->
    j + 1}), 0}, {j,
       2, 200, 2}],
    Table[{(-0.01 + 0.5 c30 form /. {jx -> j,
    jb ->
     j - 1}), 0}, {j,
       2, 200, 2}]
    ]];
While[out[[1, 1]] < loLimit, out = Drop[out,
1]];
Return[out];
    ];
showMatch[lp_, sepd_, fr_, to_, opts_, optsLP_]
:=
  Module[{lpS, i, j, pl},
   lpS = Sort[lp];
   i = 1;
   While[i <= Length[lpS] \[And] lpS[[i, 1]] <
   fr,
   i += 1];
   j = i;
   While[j <= Length[lpS] \[And] lpS[[j, 1]] <
   to,
   j += 1];
```

```
    j -= 1;
    pl = plotSeparated[sepd, fr, to, opts];
    Show[pl, ListPlot[Take[lpS, {i, j}],
    Join[optsLP,
     opts]]]
    ];
numericalFit[lbld_, pas_, jMp_, jMr_, vx_, vb_]
 :=
  Module[{da, i, lab, xy, fun, subs, gss, Nlmf},
   i = 1;
   lab = lbld;
   While[i <= Length[lab],
    If[lab[[i, 4 ;; 5]] == {vx, vb}, i += 1, lab
     =
     Delete[lab, i]]];
   xy = Transpose[Delete[Transpose[lab], {{2},
    {3},
   {4}, {5}}]];
   xy = Table[{xy[[i, 2]], xy[[i, 3]],
   xy[[i, 1]]},
   {i, Length[xy]}];
   subs = {g1 -> 0,
     g2 -> 0, \[Beta]1 -> 0, \[Beta]2 -> 0,
     \[Beta]3
     -> 0, \[Alpha] ->
       0, \[Gamma]1 -> 0, \[Gamma]2 -> 0,
       \[Gamma]3
```

```
    -> 0, \[Gamma]4 ->
    0, \[Gamma]5 -> 0, \[Omega] -> 0,
    \[Omega]x
    -> 0, \[Omega]y ->
   0, \[Omega]z1 -> 0, \[Omega]z2 -> 0,
   \[Omega]z3
   ->
   0, \[Omega]z4 -> 0, \[Omega]z5 -> 0};
fun = 0.5 c30 ((U[vb, jx + br] /. subs) -
(U[vx, jx] /. X0));
gss = {Te, Be, De, He} /. pas;
Nlmf =
 NonlinearModelFit[xy,
  fun /. Te -> gss[[1]], {{Be, gss[[2]]},
    {De, gss[[3]]}, {He,
      gss[[4]]}}, {jx, br}];
   Return[Nlmf];
   ];
removeBranch[li_, sep1_] := Module[{out, i, pos},
   out = li;
   For[i = 1, i <= Length[sep1], i += 1, {
     pos = Position[out, sep1[[i, 1]]][[1, 1]];
     out = Delete[out, pos];
     }];
   Return[out];
   ];
```

```
.....

Vlw = 3; (*Beginning*)
Vup = 7;  (*End*)
min = 337300;
max = 337310;
dat = window[min, max, 100, False];
bases = makeBases[Vup];
prange = {-100, 100};

{\[Delta]Ge, \[Delta]Be, de, he} = {0.047495 -
0.00264,
0.000108483,
   1.77168*^-8, 4.92942*^-13};
perts = {\[Delta]Ge, \[Delta]Be, de, he} +
{0, 0, 0, 0};

Manipulate[
 BL = makeSim[bases,
   perts + {\[Delta]G, \[Delta]B, \[Delta]D,
   \[Delta]H}, Vlw, Vup];
 Grid[Transpose[{{"\[Delta]G", "\[Delta]B",
 "\[Delta]D",
     "\[Delta]H"}, {\[Delta]G, \[Delta]B,
     \[Delta]D,
     \[Delta]H}}]],
 {{\[Delta]G, 0}, -0.01, 0.01}, {{\[Delta]B, 0},
```

```
 -0.0001,
  0.0001}, {{\[Delta]D, 0}, -1*^-8, 1*^-8},
  {{\[Delta]H, 0}, -1*^-13,
  1*^-13},
 ControlPlacement -> Left
 ]
Dynamic[
 Show[
  ListPlot[dat, PlotRange -> prange, ops,
  PlotStyle
  -> Red],
  ListPlot[BL, PlotRange -> prange, Joined ->
  True,
  Axes -> False],
  Frame -> True, ImageSize -> 800
  ]]

.........

low = 336500;
high = 336505;
pams = {Te -> 23394.6875, Be -> 0.0316976, De
-> 1.57*^-8,
   He -> 3.23*^-13};
(*pams=Join[{Te->23394.68501125},
nlinmf["BestFitParameters"]]; (* \
overwrite *)*)
```

```
{VX, VB} = {3, 7};
labeled = autoAssigner[listNG, pams, VX, VB,
low];
sepped1 = separator[labeled, VX, VB];
brAt = makeAttempt[pams, VX, VB, low, -2];
showMatch[brAt, sepped1, low, high, {PlotLabel
->
   "\!\(\*SubscriptBox[\(Te\), \(2\)]\) spectra
   with
   " <>
    ToString[VX] <> "-" <> ToString[VB] <>
    " band matches highlighted (" <>
    ToString[low] <>
     " to " <>
      ToString[high] <> " GHz)",
   BaseStyle -> {FontWeight -> "Bold", FontSize
   -> 14},
   PlotStyle -> {Red, Gray}, PlotRange -> {-0.2,
    1},
   Axes -> False,
   Frame -> True, ImageSize -> 700}, {PlotStyle
   -> Blue,
   Joined -> True}]
Print[Grid[
   Transpose[{{"\!\(\*SubscriptBox[\(G\),
   \(v\)]\)-Te",
      "\!\(\*SubscriptBox[\(G\), \(v\)]\)",
```

```
      "\!\(\*SubscriptBox[\(B\), \(v\)]\)",
      "\!\(\*SubscriptBox[\(D\), \(v\)]\)",
      "\!\(\*SubscriptBox[\(H\), \(v\)]\)"},
      {" ", " ", " ", " ", " "},
      SetPrecision[{Te - bases[[1]], Te, Be, De,
       He}
       /. pams, 9]}],
  Alignment -> Left]]

.........

numericalFit[lbld_, pas_, jMp_, jMr_, vx_, vb_]
:=
  Module[{da, i, lab, xy, fun, subs, gss, Nlmf},
  i = 1;
  lab = lbld;
  While[i <= Length[lab],
   If[lab[[i, 4 ;; 5]] == {vx, vb}, i += 1,
   lab =
   Delete[lab, i]]];
  xy = Transpose[Delete[Transpose[lab], {{2},
  {3},
  {4}, {5}}]];
  xy = Table[{xy[[i, 2]], xy[[i, 3]],
  xy[[i, 1]]},
   {i, Length[xy]}];
  subs = {g1 -> 0,
```

```
    g2 -> 0, \[Beta]1 -> 0, \[Beta]2 -> 0,
     \[Beta]3
    -> 0, \[Alpha] ->
       0, \[Gamma]1 -> 0, \[Gamma]2 -> 0,
        \[Gamma]3
       -> 0, \[Gamma]4 ->
       0, \[Gamma]5 -> 0, \[Omega] -> 0,
       \[Omega]x
       -> 0, \[Omega]y ->
      0, \[Omega]z1 -> 0, \[Omega]z2 -> 0,
      \[Omega]z3 ->
      0, \[Omega]z4 -> 0, \[Omega]z5 -> 0};
fun = 0.5 c30 ((U[vb, jx + br] /. subs) -
(U[vx, jx] /. X0));
    gss = {Te, Be, De, He} /. pas;
    Nlmf =
     NonlinearModelFit[xy,
      fun, {{Te, gss[[1]]}, {Be, gss[[2]]},
      {De, gss[[3]]}, {He,
         gss[[4]]}}, {jx, br}];
    Return[Nlmf];
    ];
nlinmf = numericalFit[labeled, pams, 88, 96, 3,
 7];
SetPrecision[nlinmf["ParameterTable"], 10]
ListPlot[nlinmf["FitResiduals"], Joined -> False,
 ops]
```

```
.....

frx = Transpose[nlinmf["Data"]][[1]];
brInfo = Transpose[nlinmf["Data"]][[2]];
frxP = {};
frxR = {};
ps = {};
rs = {};
For[i = 1, i <= Length[brInfo], i += 1, {
    If[brInfo[[i]] == 1,
      AppendTo[frxR, frx[[i]] + 1];
      AppendTo[rs, {i}],
      AppendTo[frxP, frx[[i]] - 1];
      AppendTo[ps, {i}];
      ];
    }];
fry = nlinmf["FitResiduals"];
fryP = Delete[fry, rs];
fryR = Delete[fry, ps];
frP = Sort[Transpose[{frxP, fryP}]];
frR = Sort[Transpose[{frxR, fryR}]];
ListPlot[{frP, frR}, PlotStyle -> {Blue, Red},
ops]
For[i = 2, i <= Length[frP], i += 1,
  If[Abs[frP[[i, 2]] - frP[[i - 1, 2]]] >
  0.012,
```

```
    Print[i, " ", frP[[i, 1]]]; i += 1]];
For[i = 2, i <= Length[frR], i += 1,
  If[Abs[frR[[i, 2]] - frR[[i - 1, 2]]] >
  0.012,
    Print[i, " ", frR[[i, 1]]]; i += 1]];
```

B $^{130}Te_2$ Linelist

Full line list to be archived for the Journal of the Optical Society of America B.

Full assigned line list to be archived for the Journal of Molecular Spectroscopy.

Line positions, half-width half-maximums (HWHM), and Areas are in the IR.

x0	HWHM	Area	v'	v"	J	P or R
664193.2802	0.00869592	0.0485126	7	11	52	1
664195.9568	0.00910404	0.0397766	7	11	44	-1
664238.2058	0.00898556	0.0337894	7	11	50	1
664240.7056	0.00648148	0.000726094	7	11	42	-1
664281.2254	0.00926288	0.0354268	7	11	48	1
664283.5518	0.00860328	0.0247104	7	11	40	-1
664322.3466	0.00828266	0.0260544	7	11	46	1
664324.5072	0.00800588	0.01114552	7	11	38	-1
664361.5672	0.00837984	0.0303112	7	11	44	1
664363.5712	0.00773734	0.00754914	7	11	36	-1
664398.888	0.00915862	0.0465764	7	11	42	1
664400.7396	0.01032156	0.041119	7	11	34	-1
664434.3122	0.00871718	0.0419352	7	11	40	1
664436.0198	0.00935558	0.0324304	7	11	32	-1
664467.8524	0.01132618	0.0851562	7	11	38	1
664469.4096	0.00854578	0.01868158	7	11	30	-1
664499.4686	0.00913736	0.0382106	7	11	36	1
664500.9106	0.0096314	0.0325906	7	11	28	-1
664529.2042	0.0087983	0.041661	7	11	34	1
664530.5248	0.00847834	0.0452666	7	11	26	-1
664557.0478	0.00854042	0.0447442	7	11	32	1
664558.2492	0.0086817	0.0225474	7	11	24	-1
664583.0002	0.00884114	0.0418186	7	11	30	1
664584.0876	0.00860672	0.025928	7	11	22	-1
664607.0614	0.00846614	0.0333384	7	11	28	1
664608.043	0.00804022	0.01286736	7	11	20	-1
664629.2322	0.00834998	0.0355178	7	11	26	1
664630.1144	0.0087015	0.023707	7	11	18	-1
664649.5166	0.00878572	0.0411388	7	11	24	1
664650.3016	0.00843444	0.0274694	7	11	16	-1
664667.9098	0.00868582	0.0240416	7	11	22	1
664668.6038	0.00841404	0.01574088	7	11	14	-1
664684.4182	0.0080481	0.01252386	7	11	20	1
664685.0266	0.0083086	0.007435	7	11	12	-1
664699.0424	0.00890396	0.029504	7	11	18	1
664699.5664	0.00878614	0.01465652	7	11	10	-1
664711.7792	0.0091986	0.0334254	7	11	16	1
664712.2254	0.00899582	0.01444612	7	11	8	-1
664722.6362	0.00853014	0.00211588	7	11	14	1
664723.0048	0.00779698	0.00158336	7	11	6	-1

x0	HWHM	Area	v'	v"	J	P or R
665695.4812	0.00756654	0.098227	3	5	48	-1
665706.0584	0.0080701	0.1033596	3	5	56	1
665742.1226	0.00761116	0.0454276	3	5	46	-1
665752.347	0.00719012	0.0350752	3	5	54	1
665786.9552	0.01172602	0.326748	3	5	44	-1
665796.819	0.00771792	0.0483734	3	5	52	1
665829.9794	0.01259372	0.307932	3	5	42	-1
665839.4762	0.00742272	0.024032	3	5	50	1
665871.199	0.00752222	0.0527472	3	5	40	-1
665880.3256	0.00663094	0.00632928	3	5	48	1
665910.607	0.0077163	0.01392652	3	5	38	-1
665919.3584	0.007214	0.0330964	3	5	46	1
665948.2084	-0.0071662	-0.0837322	3	5	36	-1
665956.5786	0.00730528	0.042966	3	5	44	1
665984.0108	0.00777684	0.05753	3	5	34	-1
665991.9942	0.0070686	0.0205886	3	5	42	1
666018.0088	0.0064612	0.001853736	3	5	32	-1
666025.601	0.0066207	0.00424046	3	5	40	1
666050.1968	0.00863426	0.229542	3	5	30	-1
666057.3952	0.00839846	0.0949782	3	5	38	1
666080.5832	-0.00774118	-0.1462966	3	5	28	-1
666087.3834	0.007833	0.1088516	3	5	36	1
666109.1664	0.00888042	0.0621496	3	5	26	-1
666115.565	0.00794802	0.085128	3	5	34	1
666135.9472	0.0082296	0.1058038	3	5	24	-1
666141.9408	0.0076431	0.0949814	3	5	32	1
666160.9234	0.00849512	0.1224024	3	5	22	-1
666166.51	0.00833218	0.0373236	3	5	30	1
666184.0984	0.007935	0.0935568	3	5	20	-1
666189.2754	0.007362	0.075574	3	5	28	1
666205.471	0.00764534	0.1558574	3	5	18	-1
666210.2344	0.00705792	0.0828034	3	5	26	1
666225.0434	0.00726106	0.1277696	3	5	16	-1
666229.3904	0.00763964	0.1089698	3	5	24	1
666242.8132	0.0069391	0.0233564	3	5	14	-1
666246.7436	0.00773288	0.122692	3	5	22	1
666258.7836	0.00871634	0.1338026	3	5	12	-1
666262.2924	0.00828596	0.1317254	3	5	20	1
666272.953	0.00926436	0.1051782	3	5	10	-1
666276.0414	0.00780152	0.1265606	3	5	18	1
666285.3204	0.00845878	0.0697076	3	5	8	-1
666287.986	0.00781304	0.1096952	3	5	16	1
666295.8866	0.00847356	0.0311866	3	5	6	-1
666298.1278	0.00771366	0.130525	3	5	14	1
666304.6534	0.00913022	0.0425694	3	5	4	-1
666306.4686	0.00784172	0.063748	3	5	12	1
666311.6178	0.00954912	0.0270556	3	5	2	-1
666313.0086	0.00833556	0.0884302	3	5	10	1
666317.7464	0.00835366	0.1173158	3	5	8	1

x0	HWHM	Area	v'	v"	J	P or R
666320.6848	0.00838862	0.0984524	3	5	6	1
666321.1576	0.00875502	0.0454784	3	5	2	1
666321.8216	0.00855458	0.0761018	3	5	4	1
670183.7504	0.00764978	0.0270856	5	9	16	1
670183.8056	0.00826162	0.01192292	5	9	8	-1
670189.5018	0.00769672	0.0409484	2	5	118	-1
670194.556	0.00551748	0.000538898	5	9	14	1
670194.588	0.0595364	0.00221774	5	9	6	-1
670199.5498	0.00738554	0.0582974	2	5	126	1
670202.1402	0.00725912	0.0576524	3	6	54	-1
670203.485	0.01027852	0.029118	5	9	12	1
670204.189	0.01123288	0.073517	3	6	62	1
670210.5278	0.01505904	0.0685026	5	9	10	1
670215.6954	0.01265172	0.0260946	5	9	8	1
670218.9882	0.01041226	0.0219102	5	9	6	1
670219.934	0.01077748	0.01527394	5	9	2	1
670220.3978	0.0133988	0.02097	5	9	4	1
670235.925	0.01168956	0.0280554	1	4	158	-1
670252.3722	0.0205038	0.0288846	1	4	166	1
670255.8164	0.01125896	0.070933	3	6	52	-1
670258.0592	0.01039826	0.0251842	3	6	60	1
670301.8884	0.011664	0.0557388	2	5	116	-1
670307.5984	0.01065598	0.0048345	3	6	50	-1
670309.9922	0.0120328	0.0560418	3	6	58	1
670312.0152	0.0128387	0.0365838	2	5	124	1
670357.4926	0.01095448	0.0869986	3	6	48	-1
670359.9994	0.01185704	0.0705162	3	6	56	1
670384.6878	0.01246984	0.01239944	1	4	156	-1
670401.5018	0.01435964	0.0115205	1	4	164	1
670405.4736	0.01164012	0.0623824	3	6	46	-1
670408.0852	0.01145192	0.0693674	3	6	54	1
670412.3664	0.00965526	0.0032868	2	5	114	-1
670422.7606	0.01047796	0.0301636	2	5	122	1
670451.5864	0.00982966	0.0235344	3	6	44	-1
670454.2574	0.01112626	0.1027868	3	6	52	1
670495.8162	0.01373678	0.216438	3	6	42	-1
670498.5248	0.0087305	0.00858772	3	6	50	1
670520.9386	0.01185432	0.000427462	2	5	112	-1
670531.5682	0.00889236	0.006528	1	4	154	-1
670538.1722	0.01071272	0.0633194	3	6	40	-1
670540.8954	0.01020164	0.0528922	3	6	48	1
670548.6714	0.00958904	0.0132124	1	4	162	1
670578.6424	0.01150938	0.0526724	3	6	38	-1
670581.3666	0.011156	0.0315576	3	6	46	1
670617.2438	0.0079185	0.041237	3	6	36	-1
670619.9308	0.01029168	0.0443414	3	6	44	1
670627.6028	0.0102988	0.0430946	2	5	110	-1
670638.4342	0.01218236	0.0024515	2	5	118	1
670653.983	0.0107184	0.0553056	3	6	34	-1

x0	HWHM	Area	v'	v"	J	P or R
670656.6274	0.01040402	0.0443682	3	6	42	1
670676.4618	0.01023292	0.0147628	1	4	152	-1
670688.8482	0.0119405	0.1035406	3	6	32	-1
670691.4364	0.01164914	0.1069204	3	6	40	1
670693.892	0.011102	0.021592	1	4	160	1
670721.8504	0.01215998	0.0982634	3	6	30	-1
670724.3668	0.01083392	0.0858816	3	6	38	1
670732.3732	0.01002052	0.069994	2	5	108	-1
670743.3728	0.0106997	0.055194	2	5	116	1
670752.9902	0.011951	0.0768702	3	6	28	-1
670755.424	0.01214846	0.1325746	3	6	36	1
670782.265	0.01240758	0.1104358	3	6	26	-1
670784.6	0.01223548	0.0915028	3	6	34	1
670809.6828	0.01291544	0.0932798	3	6	24	-1
670811.9098	0.01308176	0.1139136	3	6	32	1
670819.4852	0.00951544	0.01554338	1	4	150	-1
670835.2426	0.0104499	0.001400268	3	6	22	-1
670837.1766	0.0094358	0.00341904	1	4	158	1
670837.3514	0.01137832	0.1065494	3	6	30	1
670846.3858	0.0109908	0.0619578	2	5	114	1
670858.945	0.01391624	0.154662	3	6	20	-1
670860.9286	0.01214946	0.1035862	3	6	28	1
670880.7902	0.0136122	0.1834926	3	6	18	-1
670882.6392	0.01398808	0.1883726	3	6	26	1
670900.784	0.01242414	0.0746178	3	6	16	-1
670902.4904	0.01258034	0.271182	3	6	24	1
670918.9234	0.01373302	0.27766	3	6	14	-1
670920.481	0.01150184	0.1958054	3	6	22	1
670935.2074	0.01354202	0.165394	3	6	12	-1
670936.224	0.01055738	0.0206946	2	5	104	-1
670936.6136	0.01076912	0.0213778	3	6	20	1
670947.4854	0.01163524	0.1129816	2	5	112	1
670949.6424	0.0136229	0.219646	3	6	10	-1
670950.8876	0.01147638	0.0422724	3	6	18	1
670960.603	0.011222	0.041358	1	4	148	-1
670962.2248	0.01428302	0.212004	3	6	8	-1
670963.3062	0.01215532	0.289266	3	6	16	1
670972.9544	0.01478088	0.1513784	3	6	6	-1
670973.8694	0.0131578	0.253732	3	6	14	1
670978.5362	0.00943246	0.0360364	1	4	156	1
670981.8354	0.01101722	0.01560004	3	6	4	-1
670982.581	0.0117371	0.1974832	3	6	12	1
670988.8656	0.01021568	0.00231506	3	6	2	-1
670989.4374	0.01206478	0.0938904	3	6	10	1
670994.4408	0.01319172	0.1214276	3	6	8	1
670995.939	0.01925632	0.030876	3	6	0	1
670997.5936	0.0132246	0.1367468	3	6	6	1
670998.3418	0.01468618	0.0666348	3	6	2	1
670998.893	0.01436564	0.102498	3	6	4	1

x0	HWHM	Area	v'	v"	J	P or R
671035.3236	0.01027874	0.039047	2	5	102	-1
671046.676	0.0110296	0.076544	2	5	110	1
671099.8204	0.01056624	0.0445118	1	4	146	-1
671117.9606	0.00583822	0.001549178	1	4	154	1
671132.54	0.01174112	0.0244704	2	5	100	-1
671143.9596	0.011517	0.0338818	2	5	108	1
671227.8718	0.00960982	0.0227034	2	5	98	-1
671237.1452	0.01092282	0.01351958	1	4	144	-1
671239.3442	0.0101603	0.0201394	2	5	106	1
671255.4684	0.01235858	0.01853792	1	4	152	1
671321.333	0.01084214	0.0302052	2	5	96	-1
671332.8302	0.01006562	0.0287892	2	5	104	1
671372.5628	0.01288516	0.01169564	1	4	142	-1
671391.0608	0.00919524	0.00624972	1	4	150	1
671412.9178	0.01027276	0.01164058	2	5	94	-1
671424.4226	0.01162048	0.0348918	2	5	102	1
671502.6338	0.0100249	0.020586	2	5	92	-1
671506.0762	0.01007286	0.01285206	1	4	140	-1
671514.1296	0.00836698	0.01584488	2	5	100	1
671524.7394	0.00887688	0.00266986	1	4	148	1
671590.4782	0.0095204	0.00770338	2	5	90	-1
671601.9464	0.01076386	0.0275104	2	5	98	1
671637.726	0.01117762	0.01010288	1	4	138	-1
671656.5108	0.0095378	0.01121674	1	4	146	1
671676.459	0.00996376	0.01939722	2	5	88	-1
671687.8836	0.01101568	0.0266958	2	5	96	1
671760.5798	0.0097094	0.0247164	2	5	86	-1
671767.4884	0.0104496	0.01607884	1	4	136	-1
671771.9428	0.01000544	0.0252762	2	5	94	1
671786.373	0.01131792	0.0108309	1	4	144	1
671842.838	0.01032974	0.01649862	2	5	84	-1
671854.1268	0.01113386	0.01542146	2	5	92	1
671895.3694	0.01027114	0.015878	1	4	134	-1
671914.3414	0.01137814	0.0077461	1	4	142	1
671923.2386	0.0100868	0.01511548	2	5	82	-1
671934.4334	0.00761948	0.000359198	2	5	90	1
672001.781	0.01081488	0.0200596	2	5	80	-1
672012.8812	0.0087073	0.024163	2	5	88	1
672021.3678	0.01081468	0.01432212	1	4	132	-1
672040.2852	0.0296204	0.0290744	1	4	140	1
672078.4698	0.01071186	0.00353196	2	5	78	-1
672089.4518	0.01037592	0.0098791	2	5	86	1
672145.4922	0.01117674	0.01563088	1	4	130	-1
672153.31	0.00986466	0.0223362	2	5	76	-1
672164.16	0.01051058	0.0218308	2	5	84	1
672164.5534	0.00849312	0.001703076	1	4	138	1
672226.2928	0.0068791	0.0025977	2	5	74	-1
672237.0018	0.00803882	0.01459194	2	5	82	1
672267.7442	0.01079036	0.00578708	1	4	128	-1

x0	HWHM	Area	v'	v"	J	P or R
672286.845	0.00730634	0.00859956	1	4	136	1
672297.4156	0.01058306	0.01176158	2	5	72	-1
672307.9856	0.00761352	0.01262844	2	5	80	1
672366.7098	0.01040246	0.01256332	2	5	70	-1
672377.1196	0.00975706	0.00587192	2	5	78	1
672388.1238	0.01155974	0.00746746	1	4	126	-1
672407.1586	0.01319894	0.00687866	1	4	134	1
672434.1544	0.0103577	0.0106572	2	5	68	-1
672444.3944	0.00722312	0.01980066	2	5	76	1
672499.7508	0.0111727	0.01667246	2	5	66	-1
672506.6334	0.01110466	0.0089969	1	4	124	-1
672509.8086	0.0108117	0.00636144	2	5	74	1
672525.7442	0.01162712	0.00829782	1	4	132	1
672563.4968	0.0076015	0.01068854	2	5	64	-1
672573.376	0.01088634	0.01128798	2	5	72	1
672623.277	0.01068708	0.0080983	1	4	122	-1
672625.4158	0.0099959	0.01222994	2	5	62	-1
672634.8038	0.021819	0.000732412	6	12	126	1
672635.0708	0.01220456	0.00650388	2	5	70	1
672642.3616	0.00639386	0.00209224	1	4	130	1
672669.4468	0.01781354	0.01682356	6	12	118	-1
672685.4866	0.0098245	0.00783938	2	5	60	-1
672694.9392	0.0096106	0.00860188	2	5	68	1
672738.0602	0.00858666	0.00442422	1	4	120	-1
672743.7198	0.00872914	0.00355936	2	5	58	-1
672752.953	0.01064874	0.01411626	2	5	66	1
672755.4504	0.01200408	0.01120578	6	12	124	1
672757.1142	0.01117192	0.00762694	1	4	128	1
672789.1636	0.01119234	0.00021627	6	12	116	-1
672800.1066	0.00983742	0.001995888	2	5	56	-1
672809.1212	0.01069018	0.0133726	2	5	64	1
672850.9728	0.01046736	0.00523574	1	4	118	-1
672854.6616	0.01098234	0.01120342	2	5	54	-1
672863.4468	0.01015032	0.00891892	2	5	62	1
672869.9848	0.01114348	0.00756348	1	4	126	1
672874.0892	0.01634252	0.01791172	6	12	122	1
672906.8568	0.0101779	0.000264566	6	12	114	-1
672907.3792	0.01028756	0.00458884	2	5	52	-1
672915.9258	0.0092305	0.00458376	2	5	60	1
672958.262	0.01095772	0.01328228	2	5	50	-1
672962.0268	0.0335358	0.000957868	1	4	116	-1
672966.5612	0.01091046	0.01200288	2	5	58	1
672980.9778	0.01087494	0.0048524	1	4	124	1
672990.6232	0.01883924	0.01314018	6	12	120	1
673007.3084	0.0103344	0.000232606	2	5	48	-1
673015.3562	0.00967674	0.01511748	2	5	56	1
673022.5242	0.01736972	0.0241194	6	12	112	-1
673054.5216	0.00994604	0.01655902	2	5	46	-1
673062.3114	0.0106937	0.01805084	2	5	54	1

x0	HWHM	Area	v'	v"	J	P or R
673071.2282	0.01124158	0.01038756	1	4	114	-1
673090.0972	0.01107416	0.00927128	1	4	122	1
673099.9016	0.00864736	0.001635738	2	5	44	-1
673100.1346	0.0095957	0.00207596	3	7	100	-1
673105.0556	0.0121067	0.0118906	3	7	108	1
673105.1388	0.0084154	0.000262708	6	12	118	1
673107.4282	0.00934826	0.01431776	2	5	52	1
673136.1724	0.01622382	0.01373976	6	12	110	-1
673143.45	0.01093916	0.0240724	2	5	42	-1
673150.7072	0.01130602	0.0228284	2	5	50	1
673178.571	0.0114447	0.0059052	1	4	112	-1
673185.1678	0.01280396	0.000991426	2	5	40	-1
673192.1492	0.01153	0.021229	2	5	48	1
673196.4648	0.01142856	0.0215788	3	7	98	-1
673197.3524	0.01148046	0.00707318	1	4	120	1
673201.519	0.01132688	0.01591176	3	7	106	1
673217.6198	0.0271098	0.0247882	6	12	116	1
673225.0538	0.0106807	0.0234402	2	5	38	-1
673231.7556	0.0104283	0.01843622	2	5	46	1
673247.8004	0.01335288	0.00316794	6	12	108	-1
673263.1098	0.01032484	0.0235408	2	5	36	-1
673269.5242	0.00854112	0.01322672	2	5	44	1
673284.0606	0.01080674	0.00721312	1	4	110	-1
673290.9018	0.0112231	0.0263888	3	7	96	-1
673296.0768	0.0113858	0.0203854	3	7	104	1
673299.3384	0.0106582	0.0291288	2	5	34	-1
673302.7392	0.01110788	0.00887552	1	4	118	1
673305.467	0.0108799	0.028252	2	5	42	1
673328.0636	0.0185962	0.0203688	6	12	114	1
673333.7332	0.01076928	0.0275166	2	5	32	-1
673339.5704	0.01083312	0.0294314	2	5	40	1
673357.4194	0.01542992	0.00898208	6	12	106	-1
673366.3042	0.01091208	0.01662968	2	5	30	-1
673371.8434	0.0109929	0.0237252	2	5	38	1
673383.446	0.01099782	0.0237912	3	7	94	-1
673387.6974	0.01200122	0.0086682	1	4	108	-1
673388.7326	0.01140098	0.0227786	3	7	102	1
673397.0468	0.01203006	0.0202856	2	5	28	-1
673402.2832	0.01223566	0.0290484	2	5	36	1
673406.2612	0.01065248	0.01074114	1	4	116	1
673425.9646	0.0089394	0.0162971	2	5	26	-1
673430.892	0.01076688	0.01208734	2	5	34	1
673436.4776	0.01808176	0.0221588	6	12	112	1
673453.0488	0.01173888	0.0318688	2	5	24	-1
673457.6708	0.01142456	0.01971012	2	5	32	1
673465.0252	0.01705522	0.01771206	6	12	104	-1
673474.0982	0.01112098	0.0275172	3	7	92	-1
673478.3088	0.0113595	0.0282372	2	5	22	-1
673479.4866	0.01048268	0.0159266	3	7	100	1

x0	HWHM	Area	v'	v"	J	P or R
673482.6198	0.01091902	0.001539732	2	5	30	1
673489.4844	0.0106706	0.0100479	1	4	106	-1
673501.7422	0.01224848	0.0382034	2	5	20	-1
673505.7396	0.01155334	0.0403806	2	5	28	1
673507.9192	0.01216372	0.00923604	1	4	114	1
673523.3516	0.01246442	0.0397602	2	5	18	-1
673527.0316	0.0118724	0.0350332	2	5	26	1
673542.8626	0.0170153	0.0092572	6	12	110	1
673543.1338	0.0121802	0.0265812	2	5	16	-1
673546.4948	0.0105485	0.001973742	2	5	24	1
673561.091	0.01266274	0.0282646	2	5	14	-1
673562.8576	0.01075536	0.0205646	3	7	90	-1
673564.131	0.0125103	0.034799	2	5	22	1
673568.343	0.01127378	0.02044	3	7	98	1
673570.621	0.01670844	0.0213742	6	12	102	-1
673577.2232	0.01159714	0.01088664	2	5	12	-1
673579.9394	0.01233248	0.028026	2	5	20	1
673589.4248	0.0099958	0.00684816	1	4	104	-1
673591.5306	0.01205304	0.0223108	2	5	10	-1
673593.9214	0.0089626	0.0020516	2	5	18	1
673604.0122	0.01177294	0.0212834	2	5	8	-1
673606.0776	0.01079052	0.0380776	2	5	16	1
673607.718	0.0131365	0.008432	1	4	112	1
673614.6706	0.01447654	0.01933382	2	5	6	-1
673616.4064	0.01223568	0.0357242	2	5	14	1
673623.5018	0.01113128	0.00529854	2	5	4	-1
673624.9098	0.01133938	0.01777628	2	5	12	1
673630.5114	0.01378846	0.00687472	2	5	2	-1
673631.5874	0.01241516	0.0276936	2	5	10	1
673636.4412	0.0117387	0.024074	2	5	8	1
673637.6026	0.01378022	0.00353526	2	5	0	1
673639.0968	0.01456974	0.00618556	5	10	62	-1
673639.4682	0.01062428	0.00903116	2	5	6	1
673640.0504	0.01380672	0.00960856	2	5	2	1
673640.6718	0.0112555	0.01115142	2	5	4	1
673647.2284	0.01572142	0.01024168	6	12	108	1
673649.7276	0.00851778	0.001479928	3	7	88	-1
673655.3008	0.01065532	0.01878352	3	7	96	1
673674.2108	0.01601228	0.021437	6	12	100	-1
673687.5218	0.0107879	0.00453652	1	4	102	-1
673704.037	0.01462594	0.0243788	5	10	60	-1
673705.661	0.00692214	0.0070296	1	4	110	1
673734.7116	0.01096726	0.0287146	3	7	86	-1
673740.3622	0.01133318	0.0294978	3	7	94	1
673746.9742	0.01951942	0.01057244	5	10	66	1
673749.5686	0.01668048	0.01884774	6	12	106	1
673766.7672	0.01517796	0.00582592	5	10	58	-1
673775.7996	0.01600328	0.0208604	6	12	98	-1
673801.7384	0.0110396	0.00992628	1	4	108	1

x0	HWHM	Area	v'	v"	J	P or R
673809.4454	0.0212842	0.0233024	5	10	64	1
673817.8078	0.01102276	0.01516738	3	7	84	-1
673823.527	0.01076372	0.0218714	3	7	92	1
673827.3432	0.01585872	0.0241058	5	10	56	-1
673849.8962	0.01653992	0.0147728	6	12	104	1
673869.5628	0.01812136	0.01281802	5	10	62	1
673875.3906	0.01389424	0.00653924	6	12	96	-1
673878.14	0.00904716	0.00476068	1	4	98	-1
673885.798	0.01399222	0.01415754	5	10	54	-1
673895.9684	0.01099708	0.00719032	1	4	106	1
673899.019	0.01050746	0.0326172	3	7	82	-1
673904.7994	0.0112041	0.0275216	3	7	90	1
673927.381	-0.01321422	-0.00070238	5	10	60	1
673942.153	0.01520164	0.0235016	5	10	52	-1
673948.2074	0.01764392	0.021574	6	12	102	1
673970.7018	0.01091152	0.00928026	1	4	96	-1
673972.9778	0.01498162	0.01783742	6	12	94	-1
673978.3454	0.01017716	0.00677902	3	7	80	-1
673982.954	0.01932486	0.00815032	5	10	58	1
673984.1836	0.00767026	0.01278082	3	7	88	1
673988.343	0.01128766	0.0075607	1	4	104	1
673996.4298	0.01321208	0.0210674	5	10	50	-1
674036.326	0.01635958	0.01406524	5	10	56	1
674044.5068	0.0150076	0.0109571	6	12	100	1
674048.6476	0.01351946	0.0165584	5	10	48	-1
674055.7826	0.00857196	0.01637482	3	7	78	-1
674061.4166	0.00995588	0.00072794	1	4	94	-1
674061.6658	0.01056382	0.00925478	3	7	86	1
674068.57	0.01463614	0.0212668	6	12	92	-1
674078.867	0.01021912	0.00668058	1	4	102	1
674087.5394	0.01543938	0.00649022	5	10	54	1
674098.8428	0.01079594	0.0557132	5	10	46	-1
674131.351	0.00734228	0.028871	3	7	76	-1
674136.6322	0.01212848	0.021178	5	10	52	1
674137.2684	0.00746792	0.0391328	3	7	84	1
674138.8094	0.01269854	0.0443618	6	12	98	1
674147.0084	0.01149244	0.024515	5	10	44	-1
674150.2994	0.00853166	0.00933588	1	4	92	-1
674162.1694	0.01571476	0.01592088	6	12	90	-1
674167.5488	0.01112536	0.00556198	1	4	100	1
674183.6122	0.01527014	0.01361594	5	10	50	1
674193.1596	0.01328062	0.01376926	5	10	42	-1
674205.027	0.00701022	0.01754686	3	7	74	-1
674210.971	0.01024042	0.01305438	3	7	82	1
674228.5178	0.01090328	0.00634936	5	10	48	1
674231.0878	0.01284402	0.00803028	6	12	96	1
674237.3192	0.0128263	0.00295534	5	10	40	-1
674253.7756	0.0148563	0.0131376	6	12	88	-1
674271.3802	0.01450036	0.020409	5	10	46	1

x0	HWHM	Area	v'	v"	J	P or R
674276.8224	0.0111458	0.0314976	3	7	72	-1
674279.4924	0.01319472	0.0237216	5	10	38	-1
674282.7896	0.01188302	0.0293046	3	7	80	1
674312.2038	0.01034348	0.01801152	5	10	44	1
674319.6758	0.01448586	0.024821	5	10	36	-1
674321.3762	0.01682878	0.01848386	6	12	94	1
674322.5348	0.01167276	0.01008334	1	4	88	-1
674339.3174	0.00738794	0.01077652	1	4	96	1
674343.3886	0.0110872	0.00936062	6	12	86	-1
674346.736	0.00772046	0.0324288	3	7	70	-1
674350.9866	0.01074646	0.0256414	5	10	42	1
674352.7166	0.00739324	0.0317216	3	7	78	1
674357.8862	0.00891364	0.01670434	5	10	34	-1
674387.7782	0.01384802	0.0268274	5	10	40	1
674394.139	0.01282148	0.0238488	5	10	32	-1
674405.9	0.01038972	0.00969838	1	4	86	-1
674409.6622	0.0152265	0.0301592	6	12	92	1
674414.785	0.01067928	0.028145	3	7	68	-1
674420.7722	0.00761296	0.0272196	3	7	76	1
674422.4654	0.00520128	0.000303994	1	4	94	1
674422.5662	0.00643786	0.000563226	5	10	38	1
674428.4222	0.01201416	0.029561	5	10	30	-1
674431.0228	0.01504568	0.0442822	6	12	84	-1
674455.3576	0.0140205	0.0363834	5	10	36	1
674460.7486	0.01280758	0.0293342	5	10	28	-1
674480.949	0.01030918	0.0436272	3	7	66	-1
674486.1682	0.013435	0.000695082	5	10	34	1
674486.9316	0.01060544	0.01583088	3	7	74	1
674487.4276	0.01211302	0.00477186	1	4	84	-1
674491.1222	0.01249448	0.0214142	5	10	26	-1
674495.9452	0.01482516	0.0334518	6	12	90	1
674503.75	0.01007026	0.00487834	1	4	92	1
674515.0102	0.0134775	0.02091	5	10	32	1
674516.663	0.01442164	0.0238242	6	12	82	-1
674519.5496	0.01127108	0.0084788	5	10	24	-1
674541.881	0.00995558	0.0414606	5	10	30	1
674545.241	0.00972682	0.0605528	3	7	64	-1
674546.0256	0.00882676	0.01535	5	10	22	-1
674551.213	0.00998884	0.0164905	3	7	72	1
674566.7886	0.01109768	0.01537148	5	10	28	1
674567.1268	0.01034682	0.01118054	1	4	82	-1
674570.5548	0.0108231	0.022603	5	10	20	-1
674580.2356	0.00824398	0.001060808	6	12	88	1
674583.2036	0.0072323	0.01884036	1	4	90	1
674589.7428	0.00830086	0.0557438	5	10	26	1
674593.1446	0.01150684	0.0306824	5	10	18	-1
674600.3488	0.01236132	0.0478204	6	12	80	-1
674607.6594	0.01036852	0.087006	3	7	62	-1
674610.7328	0.01033976	0.00778618	5	10	24	1

x0	HWHM	Area	v'	v"	J	P or R
674613.6104	0.0105027	0.034399	3	7	70	1
674613.796	0.0064246	0.00081188	5	10	16	-1
674629.7808	0.01086902	0.0292936	5	10	22	1
674632.5082	0.01106022	0.0212852	5	10	14	-1
674644.9906	0.01156932	0.0348896	1	4	80	-1
674646.8742	0.01312826	0.0433322	5	10	20	1
674649.285	0.01295412	0.0335554	5	10	12	-1
674660.8072	0.01073498	0.01722618	1	4	88	1
674662.0278	0.01198372	0.0369644	5	10	18	1
674662.5318	0.01477242	0.0734834	6	12	86	1
674664.126	0.01136798	0.0292742	5	10	10	-1
674668.2056	0.01077892	0.00643376	3	7	60	-1
674674.1304	0.01071888	0.081333	3	7	68	1
674675.2374	0.01225814	0.0315816	5	10	16	1
674677.0322	0.0119221	0.0204412	5	10	8	-1
674681.9996	0.01377136	0.0293016	6	12	78	-1
674686.508	0.01227068	0.0137573	5	10	14	1
674688.0046	0.00983346	0.00992816	5	10	6	-1
674695.8396	0.01094522	0.033025	5	10	12	1
674697.0444	0.00980268	0.01108716	5	10	4	-1
674703.2344	0.01068626	0.0278622	5	10	10	1
674712.2164	0.01259268	0.00524862	5	10	6	1
674713.4644	0.01092278	0.00693262	5	10	2	1
674713.7998	0.01779492	0.0252324	5	10	4	1
674721.0254	0.0098474	0.01872522	1	4	78	-1
674726.8826	0.0098601	0.059521	3	7	58	-1
674732.7724	0.00883046	0.0478602	3	7	66	1
674736.5758	0.00999574	0.01655548	1	4	86	1
674742.8362	0.01397994	0.0387532	6	12	84	1
674761.6922	0.01401048	0.0243528	6	12	76	-1
674783.695	-0.00732872	-0.1039352	3	7	56	-1
674789.5318	0.00914742	0.0971166	3	7	64	1
674795.23	0.01011278	0.0419396	1	4	76	-1
674810.5078	0.0094529	0.0580576	1	4	84	1
674821.149	0.0133747	0.1011724	6	12	82	1
674838.6308	0.01051134	0.1800556	3	7	54	-1
674839.41	0.01362276	0.0530218	6	12	74	-1
674844.4162	0.01207588	0.340246	3	7	62	1
674867.6056	0.01050882	0.0248966	1	4	74	-1
674882.6	0.01064852	0.1229032	1	4	82	1
674891.7052	0.00989852	0.1440892	3	7	52	-1
674897.4336	-0.00636412	-0.1239314	3	7	60	1
674915.153	0.00900088	0.0365312	6	12	72	-1
674938.1594	-0.00715148	-0.0784232	1	4	72	-1
674942.9186	0.01470344	0.384136	3	7	50	-1
674948.5668	0.00839354	0.0213102	3	7	58	1
674952.8614	0.00982206	0.0976	1	4	80	1
674971.8152	0.01396052	0.24418	6	12	78	1
674988.9098	0.01292992	0.259482	6	12	70	-1

x0	HWHM	Area	v'	v"	J	P or R
674992.263	0.01126482	0.250062	3	7	48	-1
674997.8336	0.01170304	0.255422	3	7	56	1
675006.8754	0.01134508	0.0678216	1	4	70	-1
675021.2852	0.01151744	0.0417114	1	4	78	1
675039.7516	0.01121978	0.1669186	3	7	46	-1
675044.1698	0.01362808	0.1089316	6	12	76	1
675045.229	0.00969036	0.039818	3	7	54	1
675060.6938	0.01639812	0.1919896	6	12	68	-1
675073.7724	0.01108802	0.0591946	1	4	68	-1
675085.3806	0.01124088	0.1268282	3	7	44	-1
675087.8788	0.0101799	0.0246456	1	4	76	1
675090.7572	0.01118916	0.1654156	3	7	52	1
675114.543	0.01495102	0.1059608	6	12	74	1
675129.1516	0.01138904	0.1189242	3	7	42	-1
675130.5052	0.01362984	0.0637884	6	12	66	-1
675134.42	0.00846904	0.1625114	3	7	50	1
675138.8464	0.00756544	0.0562714	1	4	66	-1
675171.0682	0.01198798	0.1764328	3	7	40	-1
675176.211	0.0124302	0.148446	3	7	48	1
675182.9364	0.01110008	0.0602066	6	12	72	1
675198.3436	0.01437124	0.1928298	6	12	64	-1
675202.0884	0.01087994	0.0749794	1	4	64	-1
675211.1298	0.0116892	0.252096	3	7	38	-1
675215.5672	0.01011894	0.038311	1	4	72	1
675216.1412	0.01093124	0.203794	3	7	46	1
675249.342	0.01190604	0.212462	3	7	36	-1
675254.2116	0.01173262	0.252794	3	7	44	1
675263.5132	0.01108504	0.0688282	1	4	62	-1
675264.212	0.01331494	0.0924974	6	12	62	-1
675276.6674	0.01240144	0.043838	1	4	70	1
675285.7028	0.010628	0.206118	3	7	34	-1
675290.4208	0.01013294	0.1302098	3	7	42	1
675313.7748	0.01410956	0.1380392	6	12	68	1
675320.2182	0.01078812	0.038584	3	7	32	-1
675323.1162	0.01081934	0.0442976	1	4	60	-1
675324.7718	0.01239048	0.225152	3	7	40	1
675328.111	0.0135405	0.0997282	6	12	60	-1
675335.9388	0.01059824	0.0388122	1	4	68	1
675352.8846	0.01312436	0.1468462	3	7	30	-1
675357.2704	0.00757982	0.1959768	3	7	38	1
675376.23	0.01410888	0.138527	6	12	66	1
675380.8952	0.01016586	0.0583842	1	4	58	-1
675383.709	0.01179536	0.239134	3	7	28	-1
675387.9066	0.01113524	0.1553762	3	7	36	1
675390.0408	0.01277392	0.0798348	6	12	58	-1
675393.3846	-0.0066589	-0.00247972	1	4	66	1
675412.6928	0.01175666	0.244522	3	7	26	-1
675416.6966	0.01185622	0.178374	3	7	34	1
675436.7118	0.01229612	0.0684004	6	12	64	1

x0	HWHM	Area	v'	v"	J	P or R
675436.8574	0.00895172	0.0420038	1	4	56	-1
675439.8366	0.0130759	0.260216	3	7	24	-1
675443.6336	0.01195436	0.291608	3	7	32	1
675449.0034	0.00924172	0.0482468	1	4	64	1
675450.0024	0.01130488	0.0793044	6	12	56	-1
675465.1404	0.01224496	0.1473112	3	7	22	-1
675468.7224	0.01220342	0.0990976	3	7	30	1
675488.6078	0.00897002	0.00327654	3	7	20	-1
675490.9962	0.0112486	0.01433052	1	4	54	-1
675491.9654	0.01213002	0.0788994	3	7	28	1
675495.2162	0.01399726	0.0492078	6	12	62	1
675502.7984	0.0080382	0.00929174	1	4	62	1
675507.9964	0.0123558	0.037482	6	12	54	-1
675510.2406	0.0114019	0.047879	3	7	18	-1
675513.3626	0.00988294	0.0618086	3	7	26	1
675530.0398	0.01131324	0.096553	3	7	16	-1
675532.9196	0.01155806	0.096604	3	7	24	1
675543.318	0.01015798	0.01858314	1	4	52	-1
675548.008	0.01068232	0.01045748	3	7	14	-1
675550.6342	0.01121138	0.0676278	3	7	22	1
675551.7484	0.0127378	0.030876	6	12	60	1
675554.7624	0.0106643	0.01142716	1	4	60	1
675564.0262	0.0121656	0.00502876	6	12	52	-1
675564.1456	0.01180042	0.01525552	3	7	12	-1
675566.5122	0.01177726	0.0569892	3	7	20	1
675578.4534	0.0126141	0.0453112	3	7	10	-1
675580.5524	0.0112176	0.00257332	3	7	18	1
675590.933	0.01312322	0.0295458	3	7	8	-1
675592.755	0.0130555	0.0614278	3	7	16	1
675593.8198	0.01039044	0.0092409	1	4	50	-1
675601.5854	0.01252342	0.031775	3	7	6	-1
675603.1268	0.01109278	0.0530328	3	7	14	1
675604.9072	0.01040806	0.00725936	1	4	58	1
675606.3102	0.01211458	0.0265426	6	12	58	1
675610.4104	0.0114893	0.0184955	3	7	4	-1
675611.6638	0.01215652	0.0460778	3	7	12	1
675617.4076	0.01343238	0.00431484	3	7	2	-1
675618.093	0.01286556	0.00965774	6	12	50	-1
675618.3734	0.01211978	0.0239848	3	7	10	1
675623.2518	0.01316294	0.0373946	3	7	8	1
675624.4828	0.01379372	0.0054339	3	7	0	1
675626.3004	0.01266778	0.0268844	3	7	6	1
675626.9156	0.01342346	0.01213002	3	7	2	1
675627.5212	0.01214794	0.01836216	3	7	4	1
675642.5098	0.00995668	0.008944	1	4	48	-1
675653.2342	0.01189178	0.00552106	1	4	56	1
675658.906	0.01227102	0.0128881	6	12	56	1
675670.1994	0.00977608	0.0411396	6	12	48	-1
675689.3822	0.0063788	0.00602842	1	4	46	-1

x0	HWHM	Area	v'	v"	J	P or R
675699.732	0.01108474	0.01452788	1	4	54	1
675709.5208	0.0091603	0.0366646	6	12	54	1
675720.3342	0.0128307	0.0621316	6	12	46	-1
675734.4334	0.00665092	0.00842562	1	4	44	-1
675744.4098	0.01097372	0.01343316	1	4	52	1
675758.1808	0.0133371	0.01171974	6	12	52	1
675768.5106	0.0122428	0.01457254	6	12	44	-1
675777.666	0.00986672	0.0104248	1	4	42	-1
675787.2654	0.00875358	0.01132848	1	4	50	1
675804.8694	0.0122223	0.0190249	6	12	50	1
675814.7272	0.011726	0.0180884	6	12	42	-1
675819.0852	0.00984662	0.00608986	1	4	40	-1
675828.308	0.01055816	0.00917624	1	4	48	1
675849.5908	0.01346236	0.0208938	6	12	48	1
675858.692	0.01145604	0.00889556	1	4	38	-1
675858.9844	0.01213434	0.01349762	6	12	40	-1
675867.5278	0.010288	0.01165588	1	4	46	1
675892.3492	0.01258056	0.0276668	6	12	46	1
675896.4822	0.00960584	0.01442492	1	4	36	-1
675901.282	0.01231864	0.01100204	6	12	38	-1
675904.934	0.01111676	0.01257636	1	4	44	1
675932.4628	0.01012996	0.00236774	1	4	34	-1
675933.1428	0.00580968	0.0000747068	6	12	44	1
675940.5152	0.01048836	0.01230526	1	4	42	1
675941.6196	0.01166476	0.0205612	6	12	36	-1
675966.6334	0.01056512	0.001270734	1	4	32	-1
675971.9794	0.00911562	0.00535372	6	12	42	1
675974.2894	0.00691324	0.00623006	1	4	40	1
675980.0034	0.01098518	0.00867022	6	12	34	-1
675998.9804	0.01016528	0.00792036	1	4	30	-1
676006.2406	0.00697432	0.00930776	1	4	38	1
676008.8488	0.00904708	0.01881756	6	12	40	1
676016.4302	0.00864066	0.008083	6	12	32	-1
676029.5256	0.0068969	0.00457916	1	4	28	-1
676036.3764	0.0065881	0.00691812	1	4	36	1
676043.7548	0.0087932	0.01868702	6	12	38	1
676050.8962	-0.00521416	-0.000270796	6	12	30	-1
676058.254	0.00700828	0.00672052	1	4	26	-1
676064.6986	0.00690528	0.00855114	1	4	34	1
676076.6976	0.01241302	0.01350274	6	12	36	1
676083.3968	0.0081747	0.01114912	6	12	28	-1
676085.1664	-0.00567738	-0.0001911172	1	4	24	-1
676091.201	0.00991558	0.00996956	1	4	32	1
676107.6932	0.01007138	0.00585858	6	12	34	1
676110.2762	0.00929278	0.00443888	1	4	22	-1
676113.966	0.00965508	0.01188312	6	12	26	-1
676115.8978	0.00685176	0.00670906	1	4	30	1
676133.5578	0.00641138	0.00552186	1	4	20	-1
676136.7134	0.01148488	0.01630284	6	12	32	1

x0	HWHM	Area	v'	v"	J	P or R
676138.768	0.0105723	0.0088436	1	4	28	1
676142.556	0.01065178	0.01726686	6	12	24	-1
676155.0448	0.0111881	0.00795182	1	4	18	-1
676159.8362	0.01147306	0.0089477	1	4	26	1
676163.7864	0.0150718	0.01746864	6	12	30	1
676169.214	0.00934696	0.00291706	6	12	22	-1
676174.7186	0.01150998	0.00561926	1	4	16	-1
676179.0882	0.01166162	0.00925882	1	4	24	1
676188.9024	0.00719978	0.0001707792	6	12	28	1
676192.5848	0.00762972	0.00209906	1	4	14	-1
676193.9022	0.01026046	0.01020006	6	12	20	-1
676196.5376	0.00658794	0.00884306	1	4	22	1
676208.6308	0.01200954	0.00474124	1	4	12	-1
676212.0582	0.01230782	0.0134382	6	12	26	1
676212.1576	0.0115394	0.0080295	1	4	20	1
676216.6368	0.01327174	0.01310006	6	12	18	-1
676222.871	0.0097348	0.00290594	1	4	10	-1
676233.2598	0.01168752	0.00827818	6	12	24	1
676235.301	0.01121896	0.00278442	1	4	8	-1
676237.4212	0.0123967	0.00764374	6	12	16	-1
676237.9796	0.0102915	0.00559856	1	4	16	1
676245.9198	0.0068416	0.00111346	1	4	6	-1
676248.1712	0.0069545	0.00445622	1	4	14	1
676252.504	0.01096226	0.00523918	6	12	22	1
676254.7332	0.0189858	0.00411706	1	4	4	-1
676256.255	0.0118721	0.00985976	6	12	14	-1
676256.5608	0.01017028	0.0072493	1	4	12	1
676261.7354	0.00878394	0.001023632	1	4	2	-1
676263.133	0.00655666	0.000202092	1	4	10	1
676267.8968	0.01217174	0.00592884	1	4	8	1
676269.7982	0.01190102	0.01587038	6	12	20	1
676270.8488	0.0111664	0.00440312	1	4	6	1
676271.3256	0.01063588	0.00203588	1	4	2	1
676271.9918	0.01363392	0.00313284	1	4	4	1
676273.1338	0.01177208	0.00313478	6	12	12	-1
676285.1342	0.0122423	0.01221336	6	12	18	1
676288.0618	0.0123213	0.00204172	6	12	10	-1
676298.5178	0.01225454	0.0092783	6	12	16	1
676301.038	0.01179998	0.00448704	6	12	8	-1
676309.946	0.01128356	0.00291086	6	12	14	1
676312.0608	0.01150774	0.00428566	6	12	6	-1
676319.4216	0.01238494	0.00929492	6	12	12	1
676321.1322	0.0118929	0.0025418	6	12	4	-1
676326.9438	0.01140286	0.00843916	6	12	10	1
676328.2554	0.01497622	0.00232518	6	12	2	-1
676332.515	0.01093084	0.0070916	6	12	8	1
676336.132	0.01046312	0.0045813	6	12	6	1
676337.5084	0.00979918	0.00212322	6	12	2	1
676337.7982	0.01122324	0.00365834	6	12	4	1

x0	HWHM	Area	v'	v"	J	P or R
676309.946	0.01128356	0.00291086	6	12	14	1
676312.0608	0.01150774	0.00428566	6	12	6	-1
676319.4216	0.01238494	0.00929492	6	12	12	1
676321.1322	0.0118929	0.0025418	6	12	4	-1
676326.9438	0.01140286	0.00843916	6	12	10	1
676328.2554	0.01497622	0.00232518	6	12	2	-1
676332.515	0.01093084	0.0070916	6	12	8	1
676336.132	0.01046312	0.0045813	6	12	6	1
676337.5084	0.00979918	0.00212322	6	12	2	1
676337.7982	0.01122324	0.00365834	6	12	4	1

This volume is the property of the University of Oklahoma, but the literary rights of the author are a separate property and must be respected. Passages must not be copied or closely paraphrased without the previous written consent of the author. If the reader obtains any assistance from this volume, he or she must give proper credit in his own work.

I grant the University of Oklahoma Libraries permission to make a copy of my thesis/dissertation upon the request of individuals or libraries. This permission is granted with the understanding that a copy will be provided for research purposes only, and that requestors will be informed of these restrictions.

NAME [redacted]

DATE [redacted]

A library which borrows this thesis/dissertation for use by its patrons is expected to secure the signature of each user.

This thesis/dissertation by DAVID S LA MANTIA has been used by the following persons, whose signatures attest their acceptance of the above restrictions.

NAME AND ADDRESS DATE

Revised 10/11/2012